Rivista Italiana di Paleontologia e Stratigrafia
(*Research in Paleontology and Stratigraphy*)
vol. 127(2): 427-452. **July 2021**

A REVISION OF THE ANATOMY OF THE TRIASSIC PTEROSAUR *AUSTRIADRACO DALLAVECCHIAI* KELLNER, 2015 AND OF ITS DIAGNOSIS

FABIO MARCO DALLA VECCHIA

Institut Català de Paleontologia (ICP), Edifici ICP, Campus de la Universitat Autònoma de Barcelona, E-08193 Cerdanyola del Vallès, Spain.
E-mail: fabio.dallavecchia@icp.cat

To cite this article: Dalla Vecchia F.M. (2021) - A revision of the anatomy of the Triassic pterosaur *Austriadraco dallavecchiai* Kellner, 2015 and of its diagnosis. *Riv. It. Paleontol. Strat.,* 127(2): 427-452.

Keywords: Pterosauria; anatomy; systematics; Alps; Norian.

Abstract. Several skeletal elements preserved in the holotype and only specimen of the pterosaur *Austriadraco dallavecchiai* Kellner, 2015 (uppermost Triassic, Austria) have not been identified or have remained undescribed in previous works. They include important elements for the systematic and phylogenetic studies such as the femur, premaxillae and maxillary teeth. The broad bone initially considered the sternal plate is plausibly formed by the fused frontals, as already suggested by some authors. The diagnosis of *Austriadraco dallavecchiai* is amended on the basis of new information. The close relationship of *Austriadraco dallavecchiai* to *Seazzadactylus venieri* from the uppermost Triassic of Friuli (north-eastern Italy) is further supported by the morphological similarity between the two taxa (e.g. they share similar postorbital process of the jugal and dorsal process of the surangular).

Introduction

Pterosaurs are extinct archosaur reptiles of the Mesozoic and were the first vertebrates to evolve powered flight. Late Triassic (Norian, about 215 million years ago) pterosaurs are the oldest pterosaurs found to date, and are represented by only a handful of specimens mainly found in the Alpine region of Europe (Dalla Vecchia 2013).

The early pterosaur *Austriadraco dallavecchiai* Kellner, 2015 is based on a single specimen (BSP 1994 I 51) found in 1994 in the middle-late Norian Seefeld Formation along the western flank of the Karwendel Mountains in the Northern Calcareous Alps near the town of Seefeld in Tyrol, Austria (Wellnhofer 2003). The specimen was first reported by Wellnhofer (2001, 2003), who noticed the presence of the following skeletal elements: "isolated skull elements, both mandibular rami (incomplete) with teeth, a few isolated teeth, cervical, dorsal and caudal vertebrae, haemapophyses, ribs, gastralia, sternum, both scapulocoracoids, humeri, manual claws, a first wing phalanx, one half of the pelvis, ?femur, tibia/fibula, ?metatarsals, pedal phalanges and many bone fragments of uncertain identity" (Wellnhofer 2003: 8). Wellnhofer (2003) described and figured the jugal (Wellnhofer 2003: fig. 3A); an isolated "pseudo-unicuspid" tooth (fig. 4A) tentatively identified as a mid-maxillary tooth or alternatively as a mandibular tooth 3; an isolated unicuspid tooth tentatively identified as a rostral premaxillary tooth (fig. 4B); two partial mandibular rami with teeth (figs 5-8); cervical vertebrae (fig. 9); dorsal ribs

Received: March 16, 2021; accepted: June 07, 2021

and vertebrae (fig. 9A); a sternal plate (figs 9A and 11A); some caudal vertebrae and haemapophyses (figs 9B and 10); the scapulocoracoids (figs 9A and 12); the left humerus (figs 9A, 13 and 14B); the right wing phalanx 1 (fig. 15A); the right tibia (actually, a tibiotarsus) and fibula (fig. 15B); and a hemipelvis (identified as the left one because of the purported exposure of the acetabulum; fig. 16). A pedal ungual phalanx (see fig. 9B) is mentioned in the caption of his figure 9, but it is not described in the text. The whole specimen, preserved on "blocks I-V" (Wellnhofer 2003: 8), was also figured with an interpretive drawing (Wellnhofer 2003: fig. 2), but the small size of the image prevents the identification of the individual elements. The right humerus (preserved as an impression only; Wellnhofer 2003: 15) and two incomplete wing phalanges tentatively identified as wing phalanges 3 and 4 (Wellnhofer 2003: 16) were summarily described but not figured. Some other elements were mentioned but not described. They include "several fragments of skull bones" that are "only partly preserved, as impressions" on "blocks IV and V" and "are too fragmentary for reliable identification" (p. 8); and fragmentary long bones on "block IV" that "are probably those of radius and ulna" (p. 15). The gastralia, manual claws, ?femur, ?metatarsals, and pedal phalanges listed on p. 8 are not mentioned elsewhere in the text. Wellnhofer (2003: 7) referred specimen BSP 1994 I 51 to *Eudimorphodon* cf. *ranzii* Zambelli 1973.

In his monograph dedicated to the Triassic pterosaurs, Dalla Vecchia (2014) reported all of the bones described by Wellnhofer (2003) and figured them (figs 4.1.32-45). The unicuspid isolated tooth was identified as a one of the first and unicuspid mandibular teeth or a premaxillary tooth; the other isolated tooth described by Wellnhofer (2003) was identified as a maxillary tooth but from a more mesial position with respect to that hypothesized by Wellnhofer (2003). A cervical vertebra, identified by Wellnhofer (2003: 12) as a cervical 3 or 4, was figured in detail (Dalla Vecchia 2014: fig. 4.1.37) and reidentified as cervical 8. Five dorsal vertebrae were reported (two more than in the description by Wellnhofer). The identification of the broad triangular bone as the sternal plate by Wellnhofer (2003) was provisionally accepted, but the possibility that it may actually be another skeletal element was considered (Dalla Vecchia 2014: 88). A femur (preserved as an impression), the distal part of the left tibiotarsus, six metapodials tentatively referred as metatarsals, two small phalanges and an ungual phalanx were described (Dalla Vecchia 2014: 90) but not figured. The presence of a postorbital, part of the basicranium, two sclerotic ring elements, and a tarsal bone was also mentioned; however, these elements were not figured nor described in detail, because the declared intent of the author was to describe in detail specimen BSP 1994 I 51and name a new taxon based on it in a different paper then in progress (Dalla Vecchia 2014: 82-83). Dalla Vecchia (2014: 82) referred specimen BSP 1994 I 51 as "genus and species to be named", as it had already been done by Dalla Vecchia (2009a).

Based on BSP 1994 I 51, Kellner (2015) erected the new genus and species *Austriadraco dallavecchiai* and created for it the monospecific Family Austriadraconidae. Kellner (2015) did not identify or describe further skeletal elements or further features in the specimen BSP 1994 I 51 beyond those described and figured by Wellnhofer (2003). Kellner's only contribution to the osteology of BSP 1994 I 51 was to identify as the fused frontals the element that Wellnhofer (2003) had referred to a sternal plate (although this element is still reported as a sternum in Kellner 2015: fig. 2). However, the identification as the fused frontals by Kellner was based on Kellner's personal observation as well as on the reference to the same identification made by Bennett (2015: 801) (i.e. "Bennett in press", Kellner 2015: 676). The paper by Bennett (2015), which had been submitted for publication before Kellner (2015) and still reported the specimen as '*Eudimorphodon*' cf. *ranzii*, focused on the partial mandibular rami of BSP 1994 I 51, confirming the previous identification by Nesbitt & Hone (2010) of the more complete ramus as a right element bearing a lateral mandibular fenestra. Bennett (2015) identified the "sternum" as the fused frontals in the general description of the specimen.

Because of the publication by Kellner (2015), Dalla Vecchia did not publish his in progress paper mentioned in Dalla Vecchia (2014). Later, Dalla Vecchia (2018: fig. 3B) figured the postorbital and two sclerotic ring elements of BSP 1994 I 51. Finally, Dalla Vecchia (2019: fig. 9C) figured the basicranium of BSP 1994 I 51 and highlighted the strict relationships between *Austriadraco dallavecchiai* and the new taxon *Seazzadactylus venieri*.

Comparison with the latter taxon now allows the identification of some skeletal elements of BSP 1994 I 51 that had remained indeterminate and permits us to revise the identification of some further elements.

Here, the skeletal elements of BSP 1994 I 51 that have not been identified by Wellnhofer (2003) or Kellner (2015) nor have they been described and figured by these authors and by Dalla Vecchia (2014) are described and discussed. Furthermore, a revised diagnosis of *Austriadraco dallavecchiai* is provided.

Materials, terminology and methods

The holotype of *Austriadraco dallavecchiai* BSP 1994 I 51 is preserved on a limestone block that was broken into five fragments (numbered I to V, corresponding to blocks I-V of Wellnhofer 2003) and the counterslab of fragment IV. Fragment I contains only a small piece of bone and is not shown in Figure 1.

The specimen BSP 1994 I 51 was studied at the BSP using a binocular microscope in 2006 and 2018.

The specimens MFSN 1797, MFSN 21545 and MPUM 6009 were studied at the MFSN using a Wild M3 binocular microscope. Observation on specimens MCSNB 2886, MCSNB 2887, MCSNB 2888, MCSNB 3359, MCSNB 3496, MCSNB 8950, BNM 145124, BYU 20707 and SMNS 50735 was made personally in the Museums where they are deposited.

The term 'non-monofenestratan pterosaur' is used for all the genera once included in the Suborder Rhamphorhynchoidea of Linnean systematics (see Wellnhofer 1978), which is a paraphyletic group according to the phylogenetic systematics (e.g. Kellner 2003; Unwin 2003; and Dalla Vecchia 2009a). Enclosure in single quotation marks in the following part of the text indicates that the validity of the taxon is doubtful, or in need of a formal revision.

Following Dalla Vecchia (2009a), *Eudimorphodon ranzii* is considered to be represented only by the holotype specimen (MCSNB 2888); according to Dalla Vecchia (2018) and contra Kellner (2015), MPUM 6009 is retained in *Carniadactylus rosenfeldi*. MCSNB 8950 (*E. ranzii* for Wild 1994) does not belong to *E. ranzii* and is a distinct, still unnamed taxon according to Dalla Vecchia (2009a, 2014). The affinities of MCSNB 2887 (*E. ranzii* for Wild 1979) remain uncertain. *Raeticodactylus filisurensis* is probably congeneric with *Caviramus schesaplanensis* (see Dalla Vecchia 2009a), but the two taxa are here retained, following Dalla Vecchia (2014), and pending a formal revision based on new specimens.

The orientation of the forelimb bones is that in the flight position and the terminology used by Bennett (2001) was followed for the orientation of the bones in the space, but "cranial" and "caudal" are preferred to "anterior" and "posterior". The anatomical terminology for the skeleton is that of Romer (1956), unless specified otherwise. The terminology used for teeth and dentition in general is that used in Dalla Vecchia (2019). The tibiotarsus is the resulting element from the fusion of the tibia and the proximal tarsals.

In the drawing of the figures, tooth crowns are shaded dark grey; the bones are pale grey, whereas their impressions are white.

Institutional abbreviations – **BNM**, Bündner Naturmuseum, Chur, Switzerland; **BSP**, Bayerische Staatssammlung für Paläontologie und Geologie, Munich (Germany); **BYU**, Museum of Paleontology, Brigham Young University, Provo (USA); **MCSNB**, Museo Civico di Scienze Naturali di Bergamo "E. Caffi", Bergamo (Italy); **MFSN**, Museo Friulano di Storia Naturale, Udine (Italy); **MGUH**, Geologisk Museum - Statens Naturhistoriske Museum, Københavns Universitet, Copenhagen (Denmark); **MPUM**, Museo Paleontologico del Dipartimento di Scienze della Terra, Università di Milano (Italy); **SMNS**, Staatliches Museum für Naturkunde Stuttgart (Germany).

Systematic Palaeontology

Diapsida Osborn, 1903
Pterosauria Kaup, 1834
Unnamed clade in Dalla Vecchia, 2019
Austriadraco Kellner, 2015

Austriadraco dallavecchiai Kellner, 2015

Figs 1-7A-D, 8-12 and 14B

2001 *Eudimorphodon* cf. *ranzii* - Wellnhofer, p. 100, figure at p. 100.
2002 *Eudimorphodon* - Dalla Vecchia, p. 47.
2003 *Eudimorphodon* cf. *ranzii* - Wellnhofer, p. 7, pp. 5-22, figs 2-3A, 4-11A, 12-14B, and 15-16, tab. 1.
2003 [it] has been referred to *E.* cf. *ranzii* - Dalla Vecchia, pp. 25, 28 and 33.
2003 *Eudimorphodon* sp. - Unwin, p. 177.
2004 *Eudimorphodon* sp. - Unwin, p. 39.
2004 *Eudimorphodon* - Dalla Vecchia (2004a), pp. 50, 62 and 66, fig. 5D, tab. I.
2004 *Eudimorphodon* ... identified as *E.* cf. *ranzii* by Wellnhofer (2001), but the many osteological differences with MCSNB 2888 would suggest a different specific attribution - Dalla Vecchia (2004b), p. 19.
2006 *Eudimorphodon* - Dalla Vecchia, p. 438.
2006 *Eudimorphodon* cf. *ranzii* - Fröbisch & Fröbisch, pp. 1088-1089, fig. 5.
2008 *Eudimorphodon* cf. *E. ranzii* - Barrett, Butler, Edwards & Milner, p. 62.
2008 *Eudimorphodon* cf. *ranzii* - Stecher, pp. 196 and 200, fig. 10C, tabs 2-3.
2009 it does not belong to *Eudimorphodon* and *Carniadactylus* as well and represents a new taxon - Dalla Vecchia (2009a), p. 182, figs 3E, 4H, 11D and12, tabs 2-3.
2009 attributed to *Eudimorphodon* cf. *ranzii* Zambelli, 1973 by Wellnhofer (2003), but belongs to a new unnamed taxon - Dalla Vecchia (2009b), pp. 291 and 302, tab. 2.
2009 *Eudimorphodon* cf. *ranzii* - Butler, Barrett & Gower, pp. 1-3, fig. 1(e).
2010 referred to *Eudimorphodon* cf. *ranzii* - Nesbitt & Hone, pp. 225-226, 228 and 231, figs 1f-g and 2d.
2010 *Eudimorphodon ranzii* - Ősi, tab. 1.
2013 a yet unnamed taxon - Dalla Vecchia, pp. 129 and 133, 140-142 and 145, figs 7, 11 and 18b, tab. 1.
2014 Genere e specie da denominare - Dalla Vecchia, p. 82 and pp. 82-91, figs 4.1.32-45.
2014 *Peteinosaurus zambellii* - Hyder, Witton & Martill, fig. 4, appendix 1.
2015 '*Eudimorphodon*' cf. *ranzii* - Bennett, p. 801, fig. 8.
2015 *Austriadraco dallavecchiai* n. gen. n. sp. Kellner, p. 674 - pp. 674-677, fig. 2, tabs I-II.
2018 *Austriadraco dallavecchiai* - Dalla Vecchia, pp. 317, 320, 322-324, 330, 333 and 337, figs 1A and 3B, tab. 1.
2019 *Austriadraco dallavecchiai* - Dalla Vecchia, pp. 1-2, 11-12, 15, 20-21, 31, 38, 40-50 and 52, figs 7C, 9C, 10E-F, and 23C.

Holotype and only specimen: BSP 1994 I 51.

Distribution: middle-upper Norian (Alaunian 3-Sevatian1) Seefeld Formation of Tyrol, Austria.

Diagnosis by Kellner (2015): *Austriadraco dallavecchiai* is diagnosed by five autapomorphies and an apomorphic combination of characters within non-pterodactyloid pterosaurs.

Apomorphies are: 1) frontal with short anterior processes; 2) jugal with small maxillary and nasal processes, and a thin and elongated postorbital process; 3) presence of an external mandibular fenestra; 4) surangular dorsal process low; 5) scapula significantly longer than the coracoid (sc/co ~ 1.62). The apomorphic combination of characters is: broad coracoid with constricted shaft; deep ischiopubic plate; comparatively large tibia relative to the humerus (humerus/tibiotarsus length < 0.70) and to the wing phalanx 1 (wing phalanx 1/tibiotarsus length - 0.92).

Amended diagnosis: *Austriadraco dallavecchiai* is diagnosed by the following autapomorphies: jugal with very slender rostrodorsal (lacrimal) process which is directed rostrodorsally forming an angle of only 11° with the shorter rostroventral (maxillary) process, consequently producing a finger-like caudoventral end of the antorbital fenestra; large frontals with very narrow and long rostral (nasal) processes and a shorter and pointed rostromedian process in the plate originated from their fusion; external mandibular fenestra present; multicusped tooth crowns with 'parasite' cuspule on the larger accessory cusps; mandibular tooth 3 with distally recurved crown bearing small cuspules at the base of the mesial margin and along most of the distal margin; fan-shaped shaft of the coracoid with distally diverging margins and much broader distally than proximally; rectangular and deeper than long caudal process of ischium with the height of its distal side that is over 70% the total height of the ischium; and ischium bearing a large and ventrally directed triangular process in the ventral margin.

Integrative description of BSP 1994 I 51

Although the holotypic skeleton is disarticulated and the skeletal elements are "distributed irregularly on the surface" of the limestone block (Wellnhofer 2003: 7-8), bones from the same part of the body (i.e. skull, torso, tail, wings, etc.) are still partly associated and the original anatomical polarity is partly maintained (i.e. cranial bones are at one extremity of the specimen and caudal elements at the opposite extremity; Fig. 1). Cranial elements,

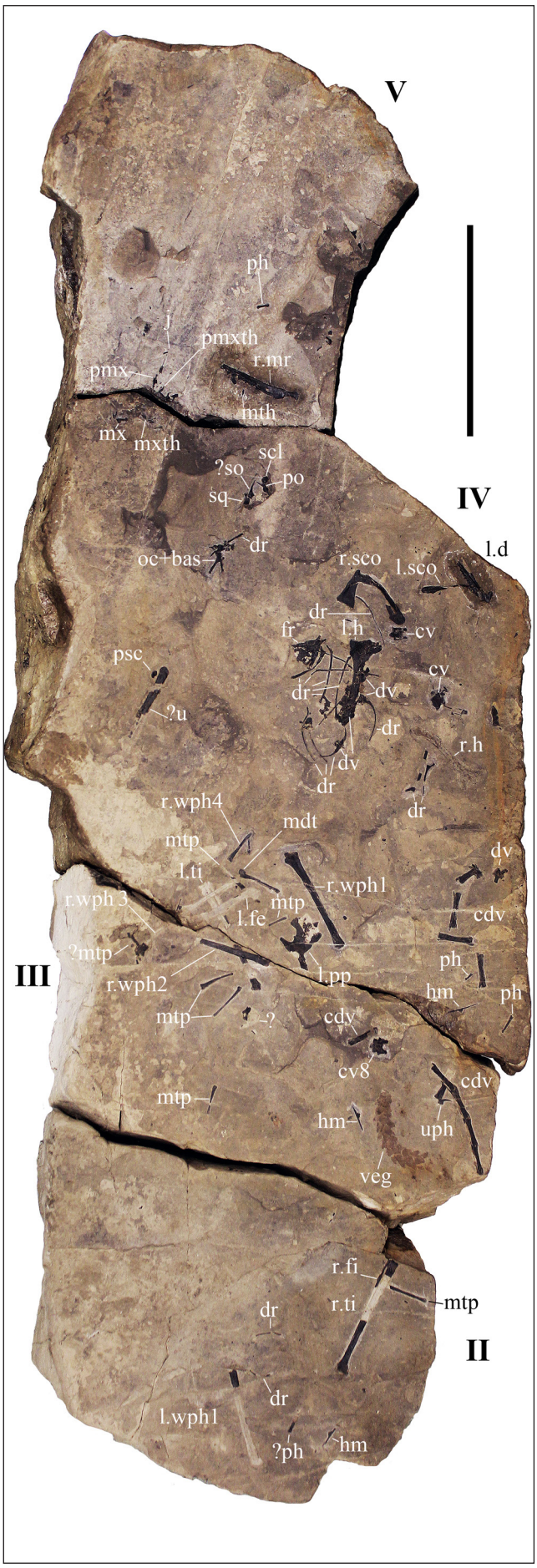

Fig. 1 - *Austriadraco dallavecchiai*, BSP 1994 I 51, holotype. Abbreviations: ?, indeterminate skeletal element; II-V, fragments II-V of the limestone block; bas, basicranium; cdv, caudal vertebra/ae; cv, cervical vertebra (cv8, cervical vertebra 8); d, dentary; dr, dorsal rib; dv, dorsal vertebra; fr, frontals; fe, femur; fi, fibula; h, humerus; hm, haemapophysis; j, jugal; l., left; mdt, medial distal tarsal; mth, mandibular tooth; mr, mandibular ramus; mtp, metapodial; mx, maxilla; mxth, maxillary tooth; oc, occiput; ph, phalanx (excluded wing phalanges and phalanges of pedal digit V; pmx, premaxillae; pmxth, premaxillary teeth; po, postorbital; pp, pelvic plate; psc, proximal syncarpal; r., right; scl, sclerotic ring elements; sco, scapulocoracoid; so, supraorbital or parietal; sq, squamosal; ti, tibiotarsus; u, ulna; veg, plant (*Brachiphyllum*); uph, ungual phalanx; wph1-4, wing phalanges 1-4. Scale bar equals 100 mm.

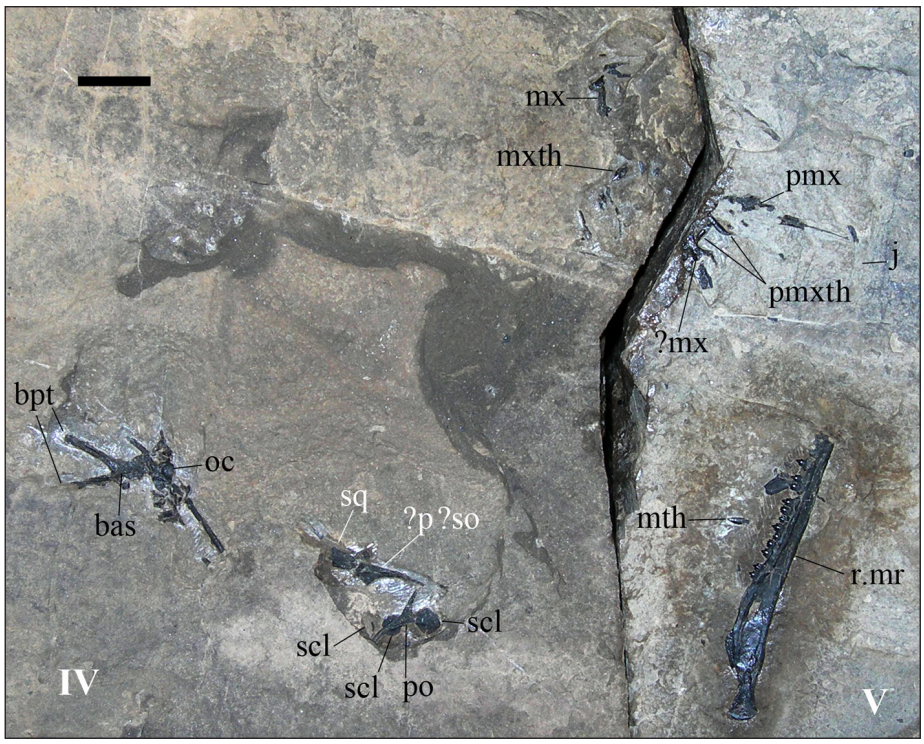

Fig. 2 - *Austriadraco dallavecchiai*, BSP 1994 I 51, holotype, skull elements. Abbreviations: IV and V, fragments IV and V; bas, basisphenoid; bpt, basipterygoid processes of the basisphenoid; j, jugal; mr, mandibular ramus; mth, mandibular tooth; mx, maxilla; mxth, maxillary tooth; oc, occiput; p, parietal; pmx, premaxillae; pmxth, premaxillary teeth; po, postorbital; r., right; scl, sclerotic ring element; so, supraorbital; and sq, squamosal. Scale bar equals 10 mm.

scattered teeth and the right mandibular ramus are clustered around the boundary between fragment IV and V (Figs 1-2). The left mandibular ramus is just slightly shifted to overlap with the close cluster including humeri, scapulocoracoids, and dorsal vertebrae and ribs in the mid of fragment IV (Fig. 1). Caudal vertebrae are grouped along the right margin of fragments III and IV (according to their orientation in Fig. 1) near the boundary between the fragments. The left hemipelvis, elements belonging to the left hind limb and four wing phalanges (presumably all from the right wing digit) also occur around the boundary between fragments III and IV, but they are clustered at the centre of the block (Fig. 1).

Skull bones

The skull elements are distributed in three closely set clusters, which are close to the right mandibular ramus (Fig. 2). The only skull element that is not preserved in these clusters is the frontal plate (see the discussion below), which is closer to the humeri, scapulocoracoids and dorsal ribs and vertebrae (Fig. 1). One cluster comprises the premaxillae, two premaxillary teeth, a jugal, part of a maxilla and putative fragments of the other maxilla, an isolated maxillary tooth and several fragmentary elements that cannot be identified. The second cluster includes a postorbital, three sclerotic ring elements, a partially preserved squamosal and perhaps a fragmentary parietal or supraorbital. The third 'cluster' is actually only part of the braincase, probably overlapped by a dorsal rib.

Premaxilla. The 19-mm-long impression of a bone located near the margin of fragment V at the boundary with fragment IV is associated with two unicuspid premaxillary teeth (see below). This skeletal element has a main body from which two processes depart bordering a deep notch; one process is short whereas the other is much longer and strap-like (Fig. 3). The latter is divided by a longitudinal line that continues into the main body. This skeletal element was erroneously identified as the second jugal by Dalla Vecchia (2014). The association with the other skull bones (Fig. 1) and with the unicuspid teeth, its shape and the comparison with the premaxillae of *Eudimorphodon ranzii* (see Wild 1979: fig. 1), *Campylognathoides liasicus* (see Wellnhofer 1974: fig. 2) and *Campylognathoides zitteli* (see Padian 2008b: fig. 2), suggest that this element represents the combined premaxillae. The longitudinal line is the dorsal boundary between the two premaxillae, the longer process is made of the two dorsocaudal (frontal) processes, the shorter process is the ventrocaudal (maxillary) process of the left premaxilla and the notch is the rostral margin of the left external naris. The dorsocaudal processes are incomplete caudally where they end against the impression of the jugal.

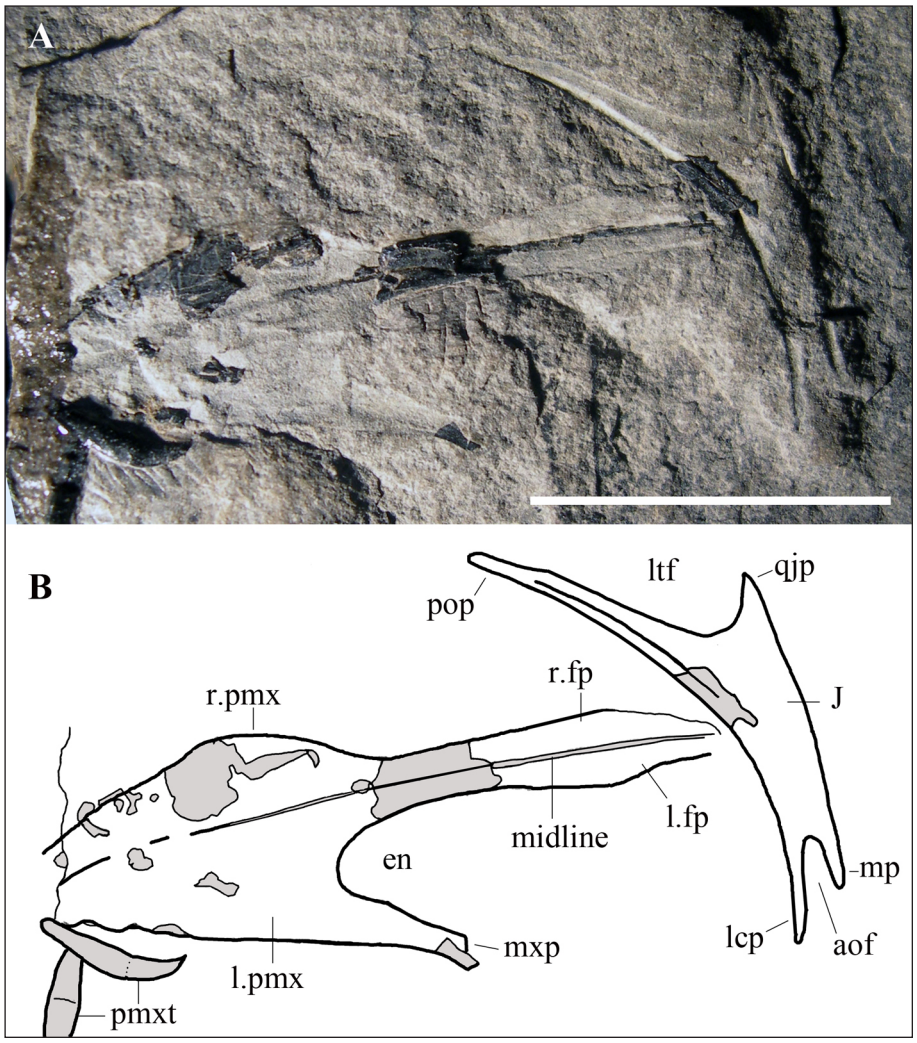

Fig. 3 - Premaxillae and jugal of *Austriadraco dallavecchiai*, BSP 1994 I 51, holotype. A) The skeletal elements as preserved; B) interpretive drawing. Abbreviations: aof, antorbital fenestra; en, external naris; fp, frontal (dorsocaudal) process of premaxilla; j, jugal; l, left; lcp, lacrimal process of jugal; ltf, lower temporal fenestra; mp, maxillary process of jugal; mxp, maxillary (ventrocaudal) process of premaxilla; pmxt, premaxillary teeth; pop, postorbital process of jugal; qjp, quadratojugal process of jugal; and r, right. The scale bar equals 10 mm.

Maxilla. Within the cluster of skull elements in the upper left corner of fragment IV in Figure 1, there is a 4 mm-long fragment of a slender and tapering bone with a single tricuspid tooth (Fig. 4). The fragment is identified as a portion of the distal part of the jugal process of a maxilla (cf. Dalla Vecchia 2019: fig. 5). Some traces of the impression of this maxilla and possibly small fragments of its premaxillary process are also preserved, but they do not allow reconstruction of the outline of the bone or the identification other significant features. Near the premaxillae on block V, there are possible fragments of the other maxilla (Fig. 2).

Jugal. The jugal was described and figured by Wellnhofer (2003: fig. 3A) and Dalla Vecchia (2014: fig. 4.1.33, 2019: fig. 7C). It is preserved as an impression close to the premaxilla (Fig. 3) and is 14 mm long. It has a peculiar shape. The main body is comparatively short and sub-rectangular. The rostroventral (maxillary) and rostrodorsal (lacrimal) processes are short and slender. The rostroventral process is rostrally directed and is parallel to the axis of the main body; the rostrodorsal process is longer than the rostroventral one and is directed rostrally and slightly dorsally (Fig. 3). These processes form an angle of only 11°. The orientation, size, shape and closeness of these processes indicate that the caudoventral end of the antorbital fenestra was narrow and finger-like. The caudoventral (quadratojugal) process is also short and triangular in lateromedial view. The caudodorsal (postorbital) process is very long (ca. 8.5 mm), slender and slightly recurved, resembling that of *Seazzadactylus venieri* (see Dalla Vecchia 2019: fig. 7); it tapers distally and probably bore a dorsocaudal facet for the articulation with the jugal process of the postorbital. The caudodorsal process is caudally inclined at about 130° with respect to the axis of the jugal body.

Frontal. A broad and plate-like skeletal element is preserved as bone in fragment IV (Fig. 5A) and as an impression in the counterslab of fragment IV (Fig. 5B). It is associated with the humeri, scap-

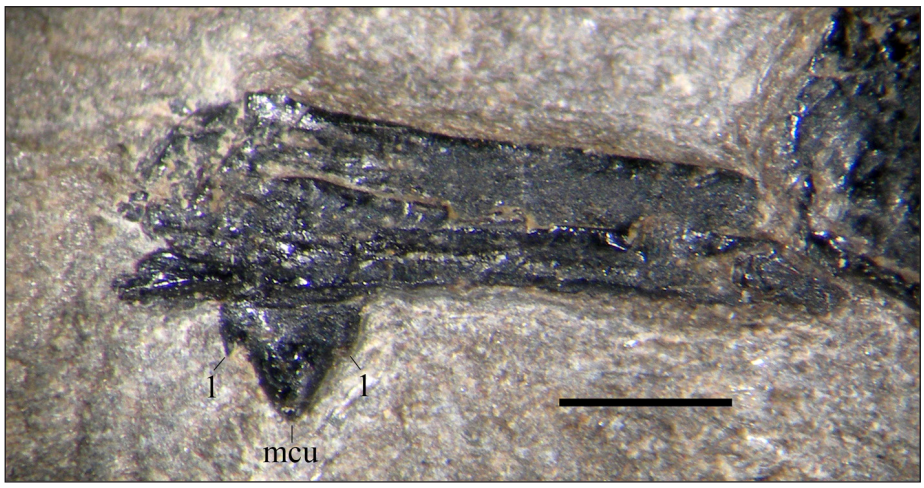

Fig. 4 - Distal fragment of the jugal process of a maxilla of *Austriadraco dallavecchiai*, BSP 1994 I 51, holotype. A tricuspid tooth is still preserved within its alveolus. Abbreviations: 1, accessory cusp 1 of the tooth; mcu, main cusp of the tooth. The scale bar equals 1 mm.

ulocoracoids and the main concentration of dorsal ribs and vertebrae of the block (Fig. 1). This bone was identified as a sternum by Wellnhofer (2003), but reinterpreted as the fused frontals by Bennett (2015: 801) and Kellner (2015: 674). The identification as the frontal plate in dorsal view is considered here the most plausible and is explained below in the Discussion section.

The element has the outline of an asymmetrical rhombus, broader caudally and narrower rostrally, with three processes at the rostral end (Fig. 5). It is ca.19 mm long from the tip of the rostrolateral processes to the caudal extremity of the plate; its maximum width is ca.13.5 mm. A thin and median longitudinal line in the caudal half of the element divides the bone into two symmetrical parts; it is the sutural line between the two frontals, which is obliterated in the rostral part of the plate. The orbital margins are slightly convex along the main body of the plate, but they become concave at the passage to the rostrolateral processes. The portions of the plate bordering the orbits are apparently thicker than the rest of the plate; these portions are narrower caudally and expand rostrally. However, their apparent thickness in the impression of the bone (Fig. 5C) is emphasized by their concavity in the actual bone as it is exposed (Fig. 5A). The portion of the element located between these two lateral and apparently thicker parts is flat and thin; its rostral part shows a grainy aspect. The caudal parietal margin has a flared V-like outline. The two rostrolateral processes are thin and elongated, straight and slightly splayed; they are the nasal processes (see Codorniú et al. 2016: fig. 1B; see Discussion). The third and rostromedian process is pointed, shorter and thicker than the rostrolateral processes and lies ventral to them (Fig. 5E-F). This rostromedian process occurs in the notch where the long caudodorsal processes of the premaxillae articulated with the frontal (Wellnhofer 1978: figs 2 and 3).

Postorbital. The postorbital is triradiate and Y-shaped (Fig. 6) with slender jugal, squamosal and frontal rami. The squamosal and frontal rami form an angle of about 80°. This indicates that the upper temporal fenestra had a somewhat acute ventrolateral margin. The frontal ramus is nearly completely covered by a sclerotic ring element. The squamosal ramus is broken distally; its preserved portion is as long as the frontal ramus. The jugal ramus is slightly recurved and is also incomplete distally. This gracile postorbital is very similar to those of specimen MPUM 6009 of *Carniadactylus rosenfeldi* (see Dalla Vecchia 2018: fig. 3A-B) and the holotype of *Seazzadactylus venieri* (see Dalla Vecchia 2019: fig. 6A).

Sclerotic ring elements. Three elements of the sclerotic ring are associated with the postorbital (Fig. 6). Two are complete and one is partially preserved. They have a subcircular outline and are very thin with a smooth surface. The association of these three elements with the postorbital shows that they did not drift away from their anatomical position as some long bones did. This supports the identification of the close elements as belonging to the same part of the skull as the postorbital.

Supraorbital or parietal: A bone preserved between the purported squamosal (see below) and the postorbital is subtriangular and slightly arched; it tapers toward one extremity (Fig. 6). Its presumed ventral margin is more curved than the presumed dorsal one. The bone is crushed and a fracture extends longitudinally along its entire body. The position of this element between the squamosal and

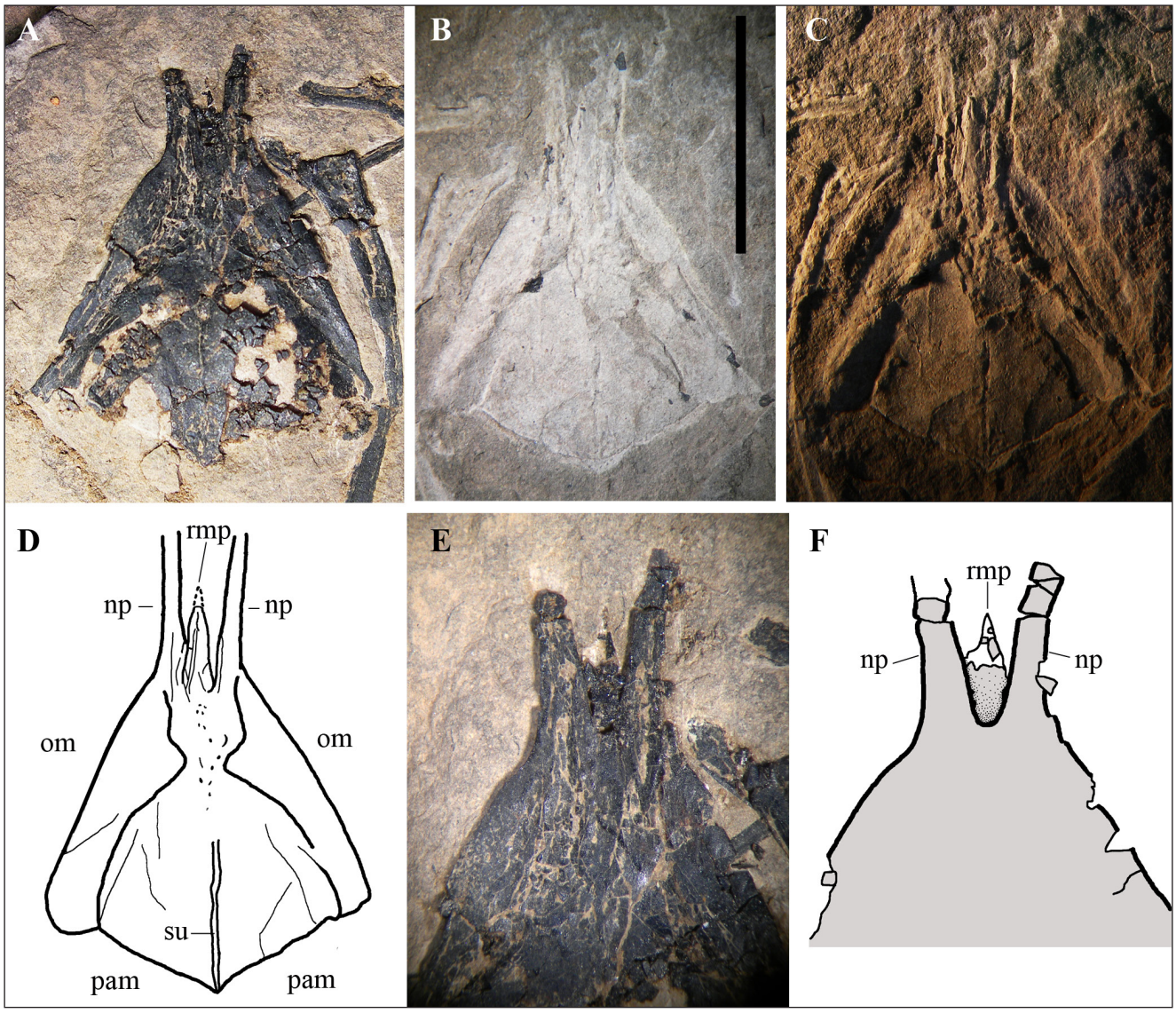

Fig. 5 - Fused frontals (frontal plate) of the holotype of *Austriadraco dallavecchiai* (BSP 1994 I 51). A) The plate as preserved on fragment IV; B) the impression of the plate on the counterslab of fragment IV; C) the impression of the plate on the counterslab with a low-angle illumination; D) interpretive drawing; E) particular of the rostral portion of the plate with the three processes; F) interpretive drawing of figure E. Abbreviations: np, nasal (rostrolateral) process; om, orbital margin; pam, parietal margin; rmp, rostromedian process; su, suture. The scale bar equals 10 mm.

the postorbital is that of the frontal or the parietal. The bone has the outline of the element that Padian (2008a: pl. 5, fig. 4) identified as the frontal in *Dorygnathus banthensis* specimen SMNS 18969. However, the frontals are broad bones in basal pterosaurs (see below) and are comparatively larger than this element. Furthermore, the fused frontals are close to the left humerus in BSP 1994 I 51. The parietal, when complete, would probably have a different shape (Wellnhofer 1975a: fig. 3a-b; Padian 2008b: figs 2, 4 and 6 and fig. 2 of pl. 7; Britt et al. 2018: fig. 3n-o). However, the bone preserved in BSP 1994 I 51 may be just a compressed fragment of the broken parietal; in that case, its ventral margin may be the dorsal margin of the upper temporal fenestra. Therefore, its identification as a parietal cannot be dismissed. An alternative identification is that of the circumorbital bone identified by Wellnhofer (1978: fig. 2), Wild (1979: fig. 1), Sangster (2003: fig. 2.3) and O'Sullivan & Martill (2017: fig. 5a) as the supraorbital and by Bennett (2014: fig. 5A) as the lacrimal. This skull bone partly borders the orbit and has a similar shape and curvature to the element under examination, although it is wider rostrally and thinner caudally and is proportionally much smaller. That appearing as the ventral margin in the element of BSP 1994 I 51 resembles an orbital margin, supporting this identification.

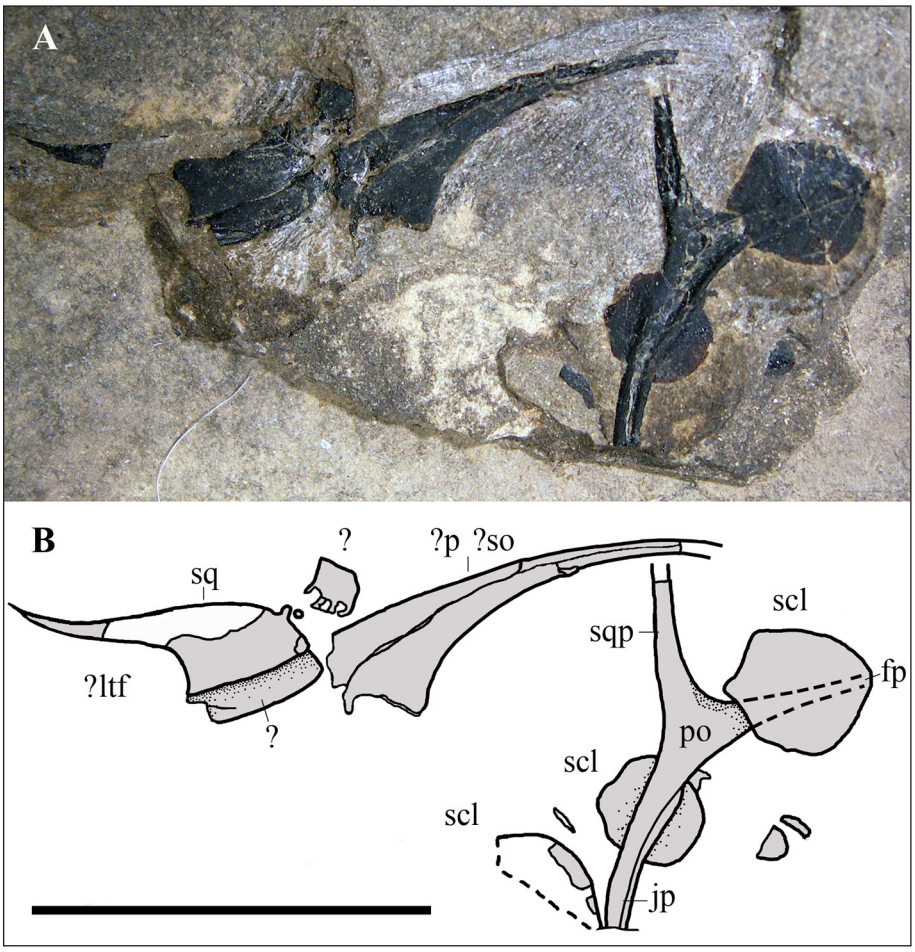

Fig. 6 - Some elements from the posterior part of the skull of the holotype of *Austriadraco dallavecchiai* (BSP 1994 I 51). A) The bones as preserved on fragment IV; B) interpretive drawing. Abbreviations: ?, indeterminate element; fp, frontal process of the postorbital; jp, jugal process of the postorbital; ltf, lower temporal fenestra; p, parietal; scl, sclerotic ring element; so, supraorbital; sq, squamosal; sqp, squamosal process of the postorbital. The scale bar equals 10 mm.

Squamosal. Another bone associated with the postorbital has a broad main body and a long and pointed process that is slightly recurved (Fig. 6). The main body is broken and incomplete and partly overlaps another broad bone, which is probably incomplete too. The squamosal is the element of the posterior part of the pterosaur skull that bears similar elongated and pointed processes (the quadrate, postorbital and parietal processes), which project from a broad main body (e.g. Wellnhofer 1975a: fig. 3a-b, 1975b: fig. 33, 1978: fig. 2; Dalla Vecchia et al. 2002: fig. 2; Padian 2008a: figs 6 and 16).

Braincase. Part of the occipital region of the braincase and the basicranium are preserved close to the squamosal, supraorbital or parietal and postorbital, in a caudal position respect to them. This portion of the skull was figured by Dalla Vecchia (2019: fig. 9C). The occipital elements are poorly preserved (they remained partly on the slab and partly on the counterslab when the rock split). The basicranium shows the basisphenoid with the slender and diverging basipterygoid processes, similar to those of *Seazzadactylus venieri* (see Dalla Vecchia 2019: fig. 9A) and other basal pterosaurs (e.g. *Carniadactylus rosenfeldi*, Dalla Vecchia 2009a: fig. 2A, 2014, fig. 4.1.103; *'Raeticodactylus' filisurensis*, Dalla Vecchia 2014: fig. 4.1.160; *Dorygnathus banthensis*, Padian 2008a: pl. 5/fig. 3, pl. 8/fig. 2, figs 12 and 17; and *Rhamphorhynchus muensteri*, Wellnhofer 1975a: fig. 3d). The basipterygoid processes are flattened in the same vertical plane as the occiput but were originally directed ventrorostrally.

Teeth

Premaxillary teeth. The isolated unicuspid tooth (Fig. 7A) was described and figured by Wellnhofer (2003: fig. 4B) and Dalla Vecchia (2014: fig. 4.1.36A). It has been tentatively identified as a rostral premaxillary tooth by Wellnhofer (2003), but may alternatively be one of the symphysial mandibular teeth (cf. *Seazzadactylus venieri*, Dalla Vecchia 2019: fig. 15A-B). As it is preserved very close to the cranial element representing the joint premaxillae (Fig. 3), Wellnhofer's identification is confirmed. Another similar but damaged premaxillary tooth is preserved close to this tooth (Figs 2-3).

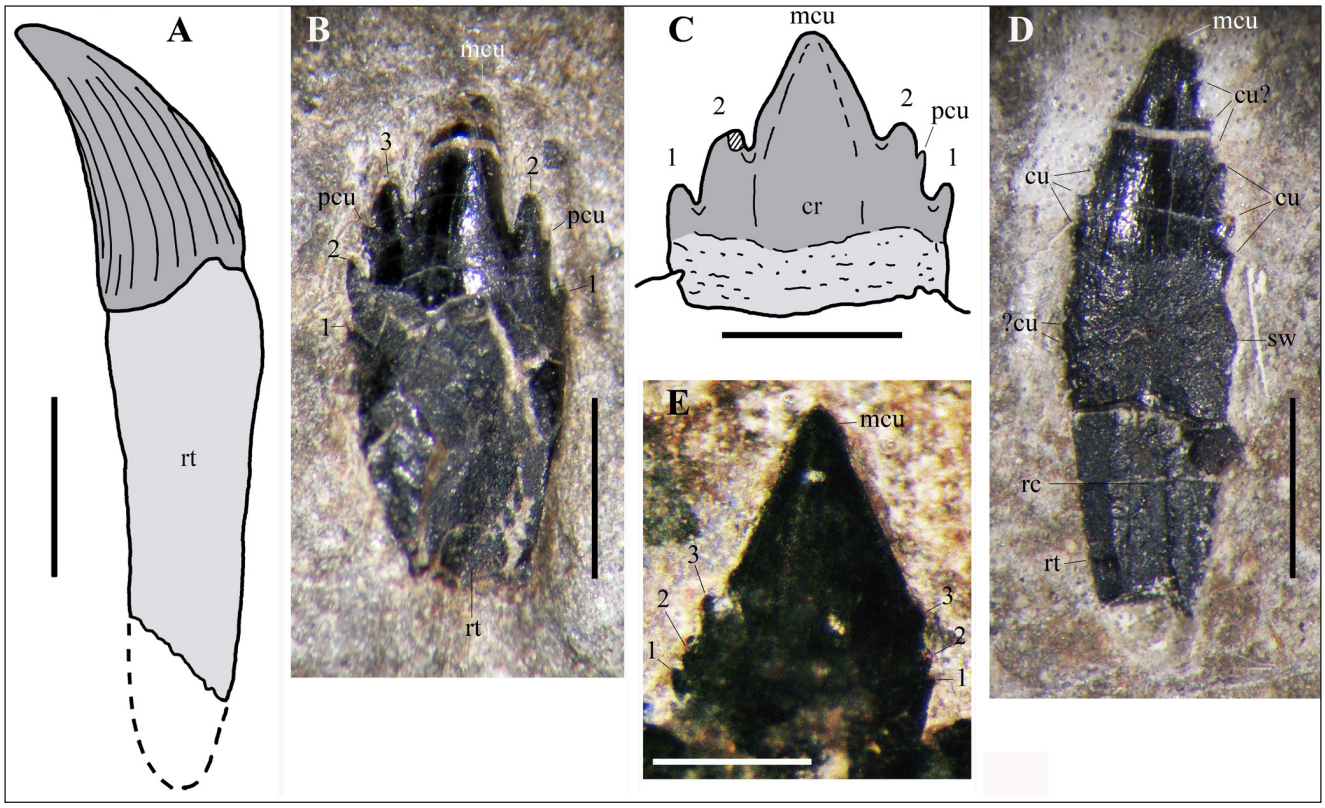

Fig. 7 - Teeth of the holotypes of *Austriadraco dallavecchiai* (BSP 1994 I 51) and *Seazzadactylus venieri* (MFSN 21545). A) Premaxillary tooth of BSP 1994 I 51; B) mesial maxillary tooth of BSP 1994 I 51; C) mid-distal mandibular tooth of BSP 1994 I 51; D) mesial mandibular tooth of BSP 1994 I 51, probably tooth 3; and E) crown of the right mandibular tooth 3 of *S. venieri,* labial view. Abbreviations: 1-3, accessory cusps 1-3; cr, crown; cu, cuspules/denticles; mcu, main cusp; pcu, 'parasite' accessory cuspule; rc, 'root' canal; rt, 'root'; and sw, swelling. The scale bar equals 1 mm in A-D and 0.5 mm in E; sizes of BSP 1994 I 51 teeth in A, C and D are those reported in Wellnhofer (2003). A and C are redrawn from Wellnhofer (2003), E is from Dalla Vecchia (2019); in A and C, the portion of the tooth covered by enamel is in dark grey.

Maxillary teeth. The crown of the tooth preserved in situ in the fragment of the jugal process of the maxilla (Fig. 4) is mesiodistally longer than basoapically high (height ~0.70 mm; height/width ratio = 0.83). It is fully erupted and tricuspid, with a large and broad main cusp and two small and pointed accessory cusps, one mesial and the other distal. The exposed crown surface is smooth. This is probably one of the distalmost maxillary teeth if not the last one (cf. Dalla Vecchia 2019: fig. 5). The distalmost teeth of the right mandibular ramus are also tricuspid (Wellnhofer 2003: figs 5-7).

An isolated tooth is preserved close to the ventral margin of the maxilla, approximately in correspondence of the presumable position of its ascending process. The tooth (crown plus 'root') is 2.7 mm high basoapically. The boundary between the crown and the 'root' is not clear but, based on the position of the first accessory cusp (Fig. 7B), the crown is about as basoapically high (~1.35 mm) as the preserved part of the 'root'. The crown of this tooth is about as high as the crowns of the largest mandibular teeth (cf. Wellnhofer 2003: fig. 7); it is higher basoapically than it is long mesiodistally (height/width ratio = 1.14). Its main cusp is much basoapically higher than mesiodistally long and slightly recurved (i.e. it is slightly asymmetrical; cf. Dalla Vecchia 2019: fig. 12B-D); the exposed side is convex and smooth. There are two accessory cusps along the distal margin and three along the mesial margin (the largest are the second and third accessory cusps, respectively; Fig. 7B), plus a small 'parasite' accessory cusp developed on the basal part of largest mesial and distal accessory cusps. Therefore, this tooth can be considered to have a total of eight cusps or to be hexacuspid if the small 'parasite' cusps are considered as parts of the largest accessory cusps. The basal accessory cusps are very small, especially the mesial one. The accessory cusps are pointed, except the most apical on both sides (i.e. the largest accessory cusps) which are somewhat blunt apically. The 'root' is

tongue-shaped and relatively short like that of the left maxillary tooth 8 of *Seazzadactylus venieri* (see Dalla Vecchia 2019: fig. 12F) and is apically damaged.

This isolated tooth is very close to the maxilla, which would support its identification as a displaced maxillary tooth. However, the mesialmost dentary teeth are not preserved in either of the mandibular rami and the multicusped mandibular teeth of his specimen can also occasionally bear 'parasite' cuspules on the main accessory cusps (Fig. 7C). Therefore, this tooth might be one of the mesialmost multi-cusped dentary teeth. An identification as a mesial maxillary tooth is suggested because of the slightly recurved main cusp, which is a feature of the maxillary crowns 2 and 3 of the closely related *Seazzadactylus venieri* (see Dalla Vecchia 2019: fig. 12B-D) and because of its short 'root'. The mesialmost multicusped dentary teeth are probably represented by the other non-unicuspid isolated tooth (see below), which lies closer to a mandibular ramus and has a different morphology.

Mesial mandibular tooth. The isolated tooth preserved close to the right mandibular ramus (Fig. 1) is nearly complete (the apex of the 'root' is represented by an impression; Fig. 7D); it is about 3.5 mm basoapically high and 0.95 mm in maximum mesiodistal length. Both mesial and distal margins of the tooth bear denticles and crenulations (Wellnhofer 2003: fig. 4A). Establishing the exact boundary between crown and 'root' is difficult in this tooth; the portion of the tooth that is covered by enamel is basoapically shorter than that not covered (it extends along the apical 36% of the tooth), but marginal crenulations or cuspules extend along the enamel-less portion (Fig. 7D). However, the crown is evidently much higher basoapically than it is mesiodistally long. The enamel is smooth, and the crown is slightly recurved distally in lateral view and flattened labiolingually. The distal cutting margin bears three cuspules which are just slightly splayed apicodistally and possibly at least two further smaller cuspules more apically (Fig. 7D; Wellnhofer 2003: fig. 4A); a swelling occurs more basally with respect to the three cuspules. The mesial cutting margin appears to bear at least three diminutive cuspules at level of the three larger distal cuspules, and possibly some further cuspules or crenulations in a more basal position (Fig. 7D; Wellnhofer 2003: fig. 4A); topographically separate elevations along the cutting margins (cuspules, crenulations and/or swellings) are less developed along the mesial margin than along the distal margin.

Wellnhofer (2003) tentatively identified this tooth as one of the large maxillary teeth set below the ascending process of the maxilla, by analogy with the condition in *Eudimorphodon ranzii* (see Dalla Vecchia 2014: figs 4.1.77B and 83), or alternatively as a mandibular tooth 3 (by analogy with specimen MPUM 6009 of *Carniadactylus rosenfeldi*; see Dalla Vecchia 2014: fig. 4.1.140A-B). Dalla Vecchia (2014: 87) considered more probable provenance from the rostral half of the maxilla, but this was before the presence of the remains of the maxilla and the nearby tooth were identified.

The crown of this tooth is no larger than those of the fully grown mid-dentary teeth, whereas the crowns of the mid-maxillary teeth of *E. ranzii* are much larger than those of the mid-dentary teeth (Dalla Vecchia 2014: figs 4.1.77B and 82). In pterosaurs, the premaxillary teeth are usually like the first mandibular teeth or at least not much different in morphology (Wellnhofer 1978: fig. 2; Dalla Vecchia 2014: figs 4.1.3A-B, 13, 82-83, 139-140A and 159, 2019: figs 3-4, 11 and 15A-B), whereas the tooth under examination is unlike the premaxillary teeth. Therefore, this tooth can be only one of the mesialmost non-unicuspid dentary teeth, which are not preserved in either of the mandibular rami, or a maxillary tooth. As noted above, a purported maxillary tooth is preserved close to the maxilla and is unlike this tooth.

Tooth 3 of MPUM 6009 differs from the premaxillary teeth and mandibular teeth 1-2 in bearing a single and small distal accessory cusp. The crown of mandibular tooth 3 of *Seazzadactylus venieri* is more similar to the crown of the tooth under examination in being much higher than mesiodistally long and bearing three mesial and three distal small accessory cusps (with distal accessory cusps that are larger than the mesial ones; Fig. 7E), although it is not recurved distally and the accessory cusps are located in the basal part of the crown only. Therefore, the tooth close to the right mandibular ramus is here identified as a mandibular tooth 3, which is transitional between the first unicuspid mandibular teeth and the following multicusped teeth with well-developed accessory cusps.

Axial skeleton

Cervical, dorsal and caudal vertebrae and dorsal ribs. Two disarticulated cervical vertebrae can be identified on fragment IV and one on fragment III (Fig. 1). The cervical vertebra close to the extremity of the right scapula shows large pneumatic foramina (Butler et al. 2009: fig. 1e; Kellner 2015: fig. 2f). The cervical vertebrae have been described and figured in Wellnhofer (2003: fig. 9) and Dalla Vecchia (2014: fig. 4.1.37).

At least four dorsal vertebrae and thirteen dorsal ribs are preserved around the left humerus and further two ribs are close by (Fig. 1; see also Wellnhofer 2003: fig. 9A and Dalla Vecchia 2014: fig. 4.1.41). A dorsal vertebra still bears the ribs articulated to its transverse processes (Fig. 1; Dalla Vecchia 2014: fig. 4.1.41). Another dorsal vertebra occurs close to caudal vertebrae on fragment IV. Two further distal dorsal ribs are located close to the isolated wing phalanx on fragment II and a rib shaft crosses the remains of the braincase. Both proximal (more robust and with large tubercula and capitula) and distal (filiform, with slender tubercula and a hint of capitula or even holocephalous; cf. Wild 1979: pl. 1) are preserved. At least 18 over a total of a possible 24 dorsal ribs (Wild 1979) occur in this specimen (i.e. 75% of the total) and most are grouped close to humeri and scapulocoracoids like in their original anatomical position. The dorsal vertebrae and ribs have been described and figured in Dalla Vecchia (2014).

There are at least ten caudal vertebrae and three isolated hemapophyses; four caudals are on fragment IV and six are on fragment III (Fig. 1). Caudal vertebrae and hemapophyses have been described and figured in Wellnhofer (2003: figs 9b and 10) and Dalla Vecchia (2014: figs 4.1.38).

Gastralia

Gastralia are rare and fragmentary in BSP 1994 I 51, with the exception of an element preserved close to and parallel with the metapodial A (see below; Fig. 11A). This gastrale has an expanded and fan-like but asymmetrical and pointed proximal portion (Fig. 11C) and a thin shaft tapering distally to a point; it seems to be the unfused half of a V-shaped median gastrale (Wellnhofer 1975a: fig. 8h; Wild 1979: pl. 2 and fig. 13; Bennett 2001: 67).

Pelvic girdle

Only an isolated and incomplete pelvic plate (hemipelvis) is preserved (partly as an impression only) in BSP 1994 I 51; it was figured by Wellnhofer (2003: fig. 16) and Dalla Vecchia (2014: fig. 4.1.44). Ilium, ischium and pubis are fused to each other without any evident suture, but the plate was unfused with the sacrum. There are no distinct facets for the articulation of the sacral ribs on this bone. Wellnhofer (2003: fig. 16) reported the circular trace of the acetabulum, which appears to be very shallow and placed rather cranially on the plate, unlike other pterosaurs. Actually, there is no rounded depression but only a craniocaudally elongated and shallow depression bordered dorsally and ventrally by a thin ridge (see Dalla Vecchia 2014: fig. 4.1.44). Thus, the identification as a left hemipelvis in lateral view is supported mainly by its proximity to elements of the left hind limb. Measuring the height of the ischiopubic plate from just dorsal to the dorsocaudal process of the ischium (see Dalla Vecchia 2014: figs 4.1.58 and 72) to the ventralmost point of the plate (excluding the ventral process of the ischium), the height/length ratio of the ischiopubic plate is 0.85. Considering the caudal process as beginning at the level of the small dorsocaudal process of the ischium, the ratio between the height of the distal side of the caudal process and the length of the entire caudal process is 1.40 and the ratio between the height of the distal side of the caudal process and the total height of the ischium (excluding its ventral process) is 0.71.

Along the ventral margin of the ischium and approximately corresponding to the beginning of the caudal process as defined above, there is a large and ventrally directed triangular process (see Dalla Vecchia 2014: fig. 4.1.44).

The surface of the pelvic plate has a grainy aspect like that of the scapulocoracoid; together with the lack of fusion of the pelvic plate to the sacrum, it provides further evidence of immaturity of BSP 1994 I 51.

Limb bones

Radius and ulna. Wellhofer (2003: 15) wrote that "fragments of other long bones [of the wing skeleton, excluding left humerus and right wing phalanx 1] are probably those of radius and ulna, and of some distal wing phalanges". The distal wing

phalanges are two incomplete bones on fragment IV identified as wing phalanges 3 and 4 (Wellhofer 2003: 16; see below). Only three fragmentary long bones in BSP 1994 I 51 can be candidates for a radius or ulna (Fig. 1). One of these (Fig. 8A) overlaps the left tibiotarsus at the boundary between fragments III and IV; the second (Fig. 8B) is preserved isolated at the extremity of fragment II; and the third (Fig. 8C) is isolated on fragment IV, to the left of the humeri in Figure 1. Only the last could be identified as a radius or ulna. Its distal portion is mostly preserved as bone, whereas the proximal third is represented only by the impression of the bone. This element appears to be relatively stout, but its proximal extremity is not clearly identifiable and the bone could be slightly longer than shown in Figure 8C. The preserved part is ca. 38 mm long. The shaft is straight, with the minimum width at mid-shaft, and slightly expands at the extremities. The distal end of the bone has a rounded and nearly symmetrical outline. This is probably an ulna, because the ulna is more robust than the radius, it has a more expanded proximal part, and its distal expansion is nearly symmetrical in early pterosaurs, whereas that of the radius is markedly asymmetrical with a large cranial tubercle (Wild 1975: figs 3-4; Sangster 2003: fig. 3.7; Dalla Vecchia 2014: figs 4.1.93 and 4.1.113C, 2018: fig. 4). However, the right wing phalanx 1 of BSP 1994 I 51 also has a nearly symmetrical distal end (Fig. 8D). The presence of a proximal syncarpal close to the bone under examination (Fig. 8C) and the probable presence of the left wing phalanx 1 elsewhere on the block (Figs 1 and 8B) supports its identification as an ulna rather than a wing phalanx.

Carpus. The small bone preserved close to the distal end of the ulna (Fig. 8C) shows two elliptical depressions that resemble the ulnar and radial facets on the proximal side of the proximal syncarpal (cf. Wellnhofer 1975a: fig. 12b-e). Therefore, it is identified here as the proximal syncarpal in proximal view. This bone is comparatively small (3.7 mm) and may be incomplete.

Wing phalanges. Wellnhofer (2003: 16) identified a wing phalanx 3 and a wing phalanx 4 in fragment IV, but it is unclear to which of the several long bones clustered around the boundary between fragments III and IV (Fig. 9) he referred to.

A long, slender and straight bone preserved partly on fragment III (proximal part) and partly on fragment IV (distal part; Figs 1 and 9) is evidently a wing phalanx. Only a part of the proximal extremity of this wing phalanx is preserved as bone, whereas the rest of the element is represented by an impression. The proximal end of the phalanx is damaged and the impression of the distal end is missing; furthermore, part of the impression at mid-shaft is missing because of the fracture between fragments III and IV. The preserved portion of this wing phalanx is ca. 55 mm long. The proximal part is expanded and slightly recurved; the shaft is straight and tapers slightly distally. This wing phalanx is much thinner than wing phalanx 1 and comparison with wing phalanges of other Triassic pterosaurs suggests it is a wing phalanx 3 (Wild 1979: pl. 14; Padian 1980: fig. 2; Wild 1994: figs 2 and 4; Stecher 2008: fig. 5; Dalla Vecchia 2014: fig. 4.1.20, 4.1.96 and 97A, 4.1.119, 4.1.132A, 4.1.164, 4.2.3, 4.2.5 and 4.2.12; and 2019: fig. 22). It is probably the right wing phalanx 3 because of its association and spatial relationship with the right wing phalanx 1 and the other wing phalanges (Fig. 9). As the preserved portion is longer than the entire wing phalanx 1, wing phalanx 3 is longer than wing phalanx1 in BSP 1994 I 51, as in *Preondactylus buffarinii*, *Peteinosaurus zambellii*, MCSNB 8950, *'Raeticodactylus' filisurensis* and *Seazzadactylus venieri* and unlike *Carniadactylus rosenfeldi* and *Campylognathoides* spp. (Dalla Vecchia 2014: 306, 2019: tab. S1).

Between the right wing phalanges 1 and 3, there is a long bone (Figs 8A and 9) in the position that would be occupied by the right wing phalanx 2, if the right wing digit is only slightly disarticulated (cf. Stecher 2008: fig. 5; Dalla Vecchia 2009a: fig. 1, 2019: fig. 1). This bone is incomplete distally; the preserved part is 37.5 mm long. The proximal portion of the bone is slightly flared in dorsoventral view as is typical of the wing phalanges and bears a concave proximal articular facet. The shaft is straight and tapers slightly distally, but it starts expanding again at the distal end of the preserved portion. This long bone is not an ulna or radius because of the flared extremity and the tapering shaft. It is less robust than wing phalanx 1 and more robust than wing phalanx 3, therefore it is plausibly the right wing phalanx 2.

The long bone that is preserved isolated at the extremity of fragment II (Fig. 8B) is also a wing phalanx. It is incomplete proximally and is mostly represented by the impression of the bone. The pre-

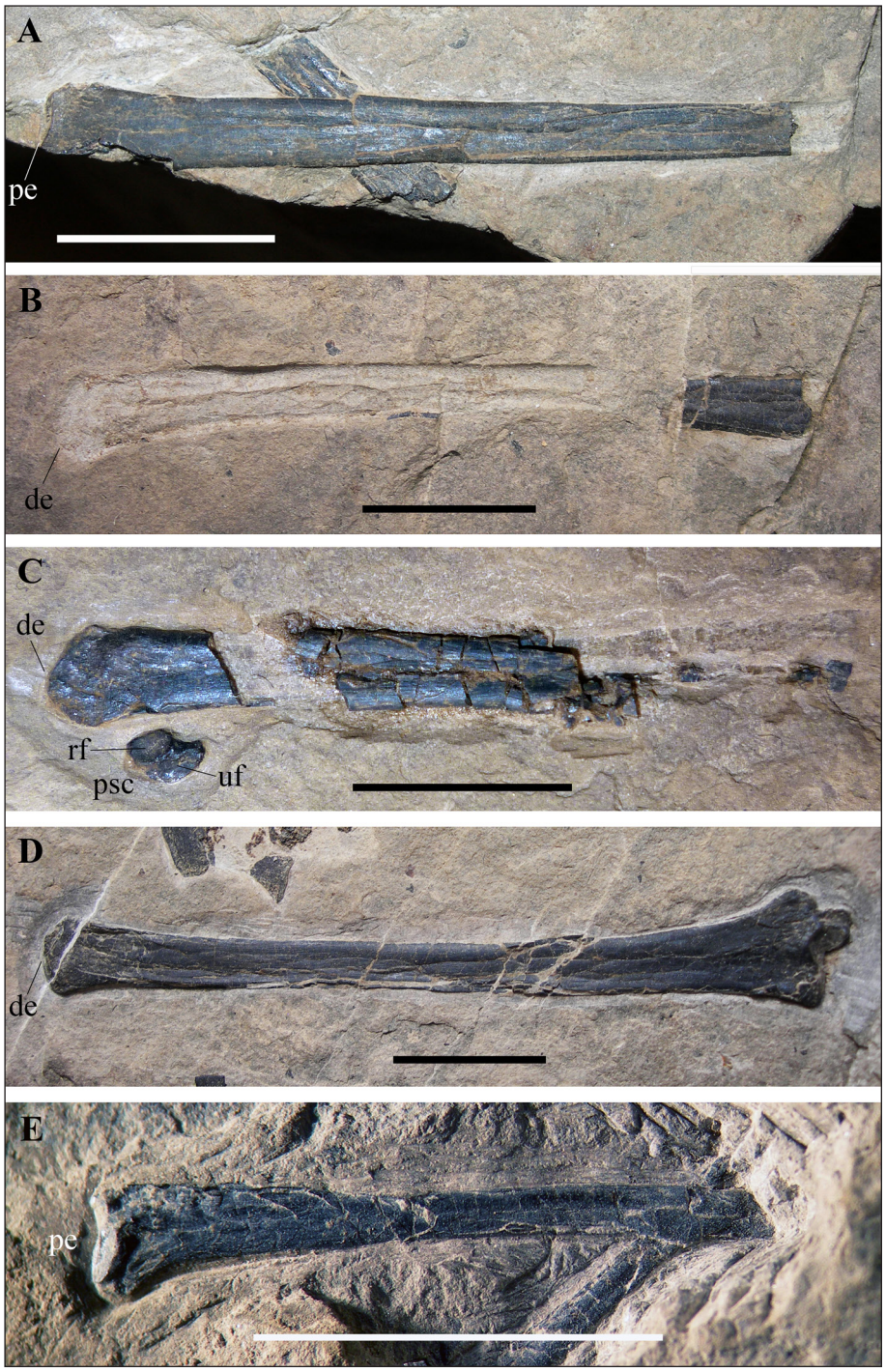

Fig. 8 - Wing phalanges, ulna and proximal syncarpal of the holotype of *Austriadraco dallavecchiai* (BSP 1994 I 51). A) The right wing phalanx 2, preserved on fragment III; B) the left wing phalanx 1, fragment II; C) the ulna with the proximal syncarpal, fragment IV; D) the right wing phalanx 1, fragment IV; E) the right wing phalanx 4, fragment IV. Abbreviations: de, distal extremity; pe, proximal extremity; psc, proximal syncarpal; rf, radial facet of the proximal syncarpal; uf, ulnar facet of the proximal syncarpal. The scale bars equal 10 mm.

served part is 46.5 mm long. Its distal end is expanded and slightly asymmetrical. The shaft is narrower at mid-shaft, expands toward the extremities and is slightly recurved. Size, robustness, curvature and the slightly asymmetrical distal expansion suggest that it is the left wing phalanx 1 (cf. Figs 8B and D).

Wing phalanx 4 is usually the shortest and most gracile of the wing phalanges (Dalla Vecchia 2014: 306). The purported wing phalanx 4 identified by Wellnhofer (2003) is probably a bone still covered by matrix in its distal part (Figs 8E and 9-10). The exposed portion is straight and its proximal extremity is flared in dorsoventral view and markedly asymmetrical. Its proximal face bears a depressed articular facet, which suggests this is the smallest wing phalanx rather than a metapodial.

Femur. The impression of a femur (Fig. 10) crosses the proximal part of left tibiotarsus along the margin of fragment IV near the pelvic plate (Figs 1 and 9). If it is the left femur, as its association with the tibiotarsus and the pelvic plate suggests, it was exposed in caudal view and that preserved is

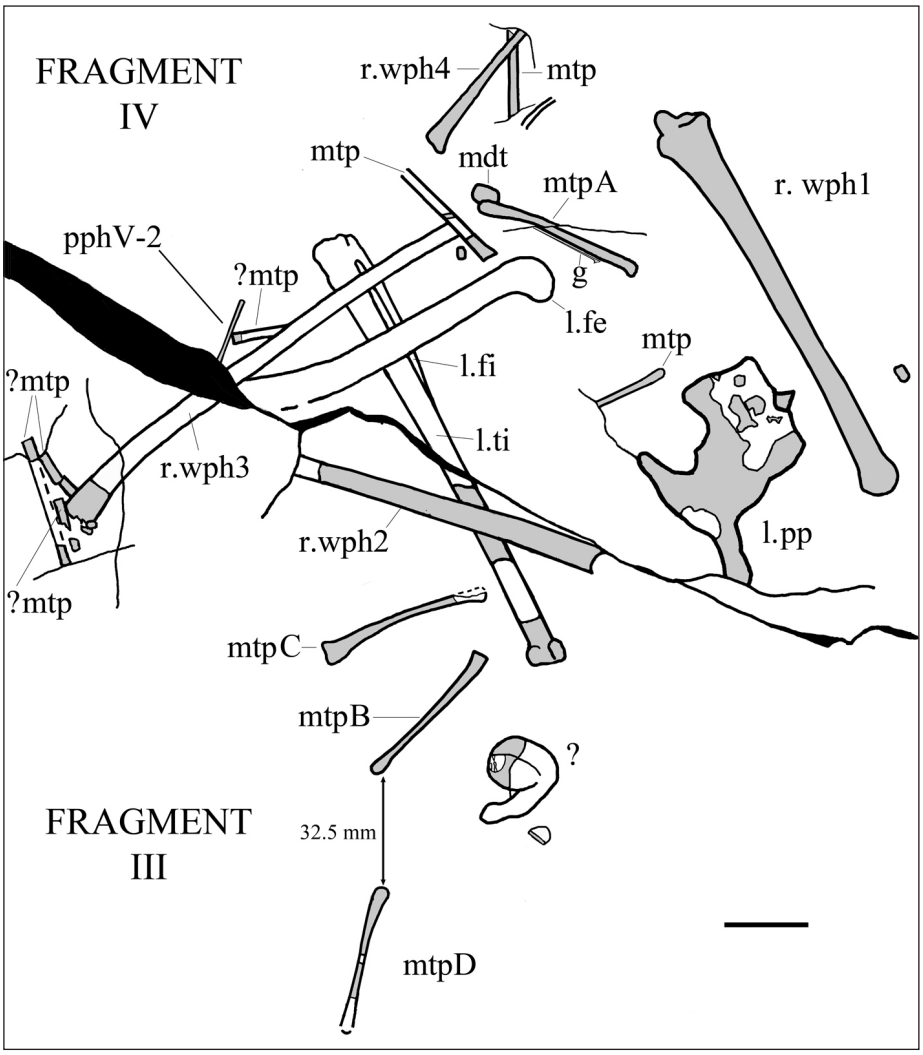

Fig. 9 - Limb bones of the holotype of *Austriadraco dallavecchiai* (BSP 1994 I 51) along the boundary between fragments IV and III. Abbreviations: ?, indeterminate skeletal element; fe, femur; fi, fibula; g, gastrale; l., left; mdt, medial distal tarsal; mtp, metapodial; pp, pelvic plate; pphV-2, pedal phalanx V-2; r., right; ti, tibiotarsus; wph1-4, wing phalanges 1–4. The better preserved metapodials are indicated with capital letters. The metapodial D is located 32.5 mm from metapodial B (see Figure 1); this distance was shortened in the figure for graphic reasons. The scale bar equals 10 mm.

the impression of its cranial side. The impression is nearly complete, lacking just the distal extremity of the distal condyles, and is 37.5 mm long. The femur is sigmoid and the caput femoris is bent at 130°-135° as that of the holotype of *Preondactylus buffarinii* (see Dalla Vecchia 2014).

Tibiotarsus and fibula. Neither Wellnhofer (2003) nor Kellner (2015) reported the coosified left tibiotarsus and fibula, which are preserved partly on fragment IV and partly on fragment III (Figs 1 and 9-10). Only portions of the distal half of this composite element and a segment of the shaft of the fibula are preserved as bone, whereas the rest is represented by the imprint of the bone. No further features can be observed with respect to the right element, which is preserved on fragment II (Fig. 1).

Distal tarsals, metapodials and phalanges of pedal digit V. At least 11 scattered, thin and long skeletal elements occurring in the cluster of pelvic, hind limb and wing finger bones located along the boundary between fragments III and IV (Figs 9 and 11A-F) could be metapodials or pedal phalanges V-1 and 2 (the latter have a metapodial habitus in Triassic pterosaurs; Dalla Vecchia 2014). One further incomplete metapodial is preserved close to the right tibia (Figs 1 and 11G). Most of these are incompletely preserved or are still partly covered by rock. The better preserved of these bones have been arbitrarily indicated with a capital letter in Figure 9 to ease their description. The presence of mixed long bones from one hind limb and one forelimb in the cluster and the high number of potential metapodials (one pes had four elongated metapodials and two pedal phalanges in digit V) would suggest a mixture of manual and pedal metapodials. Unfortunately, it is difficult to distinguish between disarticulated metacarpals and metatarsals, mainly when their extremities are not preserved and their total length is unknown.

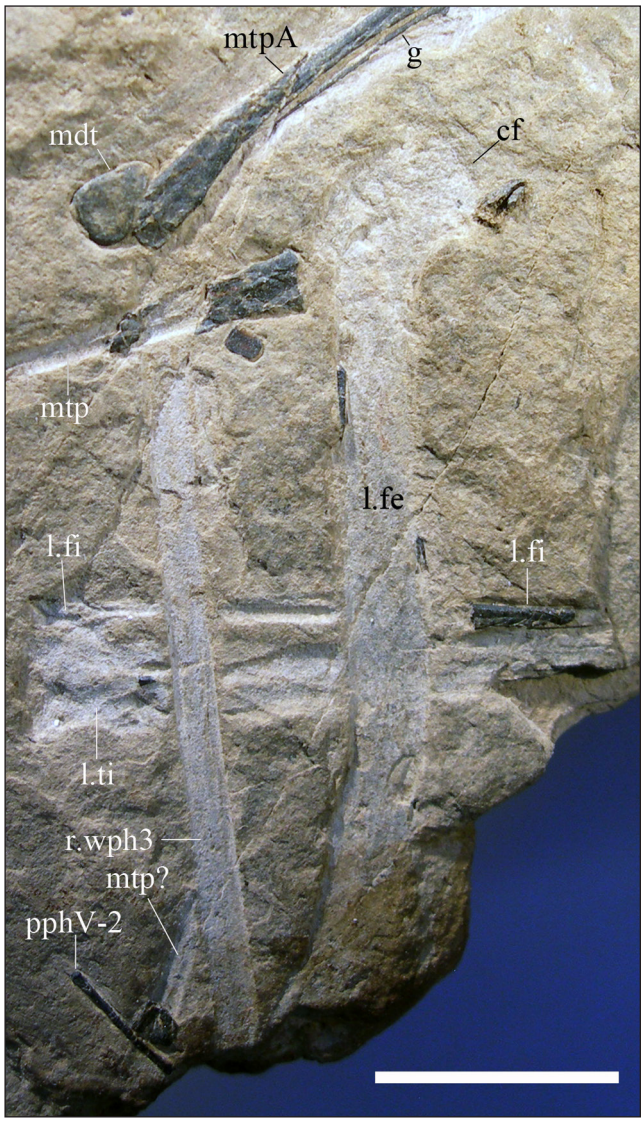

Fig. 10 - Left femur and other limb bones of the holotype of *Austriadraco dallavecchiai* (BSP 1994 I 51). Abbreviations: cf, caput femoris; fe, femur; fi, fibula; g, gastrale; l., left; mdt, medial distal tarsal; mtp, metapodial; mtp A, metapodial A (possibly metatarsal II); pphV-2, pedal phalanx V-2; r., right; ti, tibiotarsus; wph3, wing phalanx 3. Scale bar equals 10 mm.

None of the bones under examination can be unequivocally identified as phalanges of pedal digit V (cf. Padian 1983: fig. 22; Sangster 2003: fig. 3.22; Dalla Vecchia 2014: figs 4.1.69A, 97B-C, 101 and 130), except a thin and straight element close to the impression of wing phalanx 3 (Figs 9-10) which could be a pedal phalanx V-2. This bone lacks one extremity and is slightly constricted at mid-shaft; the preserved extremity is blunt and slightly expanded. Although this element is as thin and straight as a gastrale, gastralia are usually pointed at both extremities (Wellnhofer 1975a: fig. 8h; Wild 1979: pl. 2 and fig. 13).

The metapodials preserving their complete outline (metapodials A-D in Fig. 9) have an expanded proximal portion, a slender shaft that tapers up to the middle and then gradually expands toward a distal articular region that is moderately enlarged. Metapodial A (Fig. 11A) is completely preserved as bone and is slightly recurved. It is 21 mm long. Its proximal portion is expanded and club-like and still contacts a small flat bone with an oval outline (Fig. 11A-B). The distal end of this metapodial bears a bicondylar ginglymus with small and crushed condyles (Fig. 11C). Metapodial B (Fig. 11D) is also completely preserved as bone and is 19 mm long. Its proximal portion is expanded fan-like and recurved, whereas the shaft is straight. The distal portion of metapodial C is preserved as an impression of the bone (Fig. 11E). This metapodial is recurved and its proximal portion is expanded fan-like, like that of metapodial B. Its total length is 20.5 mm. Metapodial D (Fig. 11F) lacks its proximal portion, which is represented by the impression of the bone. It is straight and its proximal and distal extremities (Fig. 11H) appear to be similar to those of metapodial A. Its total length is 18 mm, thus it is smaller than metapodials A-C.

The metapodial preserved near the right tibiotarsus (Fig. 11G) lacks its proximal portion. The preserved part is also 19 mm long. It is straight and its distal extremity (Fig. 11J) is similar to that of metapodial D.

Because of the shape of its proximal portion and shaft curvature, metapodial A resembles the metatarsal of *Dimorphodon macronyx* figured by Padian (1983: fig. 14a), which he identified as metatarsal II. For the same reason, however, it is also similar to metatarsal I of specimen MCSNB 3359 (Dalla Vecchia 2014: fig. 4.1.69A-B) and MCSNB 3496 (Dalla Vecchia 2014: figs 4.1.73) of *Peteinosaurus zambellii* and to metatarsal I of *Carniadactylus rosenfeldi* holotype (see Dalla Vecchia 2009a: fig. 9, 2014: fig. 4.1.101A and C). The small oval bone contacting metapodial A is most probably a mesopodial element. Two mesopodials contact the metatarsals in pterosaurs: the lateral and the medial distal tarsals. The lateral distal tarsal has a rectangular outline and is constricted in the middle in proximal and distal views (Padian 1983: fig. 20; Dalla Vecchia 2014: figs 4.1.69B and 70); instead, the medial distal tarsal is flat and roughly quadrangular in the same views (Padian 1983: fig. 12d). Metatarsal I articulates on the medial

Fig. 11 - Metapodials of the holotype of *Austriadraco dallavecchiai* (BSP 1994 I 51). A) Metapodial A (possibly metatarsal II); B) metapodial A, detail of the proximal portion with the medial distal tarsal; C) metapodial A, detail of the distal end; D) metapodial B, possibly metatarsal I; E) metapodial C, possibly metatarsal III; F) metapodial D, possibly metatarsal IV; G) the metapodial near the right tibiotarsus, possibly also a metatarsal II or III; H) metapodial D, detail of the distal end; I) metapodial near the right tibiotarsus, detail of the distal end. Abbreviations: g, gastrale; mdt, medial distal tarsal. Scale bars equal 5 mm.

distal tarsal, as does metatarsal II. This mesopodial element is plausibly a medial distal tarsal, probably showing its proximal aspect, as only a large shallow depression can be seen instead of the three facets for metatarsals I-III (Padian 1983: fig. 20). Therefore, metapodial A may be a metatarsal I or II.

Metapodials B-C are close to the left tibia and may belong to the disarticulated left pes; metapodial D may be from the same pes (Fig. 9). Metatarsals IV<I<III<II in MFSN 1797 (*Carniadactylus rosenfeldi*), MCSNB 3359 (*Peteinosaurus zambellii*) and MCSNB 8950 (Dalla Vecchia 2014), and IV<I<II<III in *Dimorphodon macronyx* (Sangster 2003: appendix 1). According to these proportions, metapodials B-D could be from the same pes and metapodial C would be metatarsal II or III, as metapodial D<B<C. In this case, metapodial A could not be metatarsal I, because metatarsal I is always shorter than metatarsals II and III. In the pedes of MFSN 1797, the metatarsals (mt) are longer than the metacarpals (mc): mcI-III are 13.7, 17.2 and 19.2 mm long, while mt I-IV are 20.5, 22, 21 and 19.5 mm long, respectively. MFSN 1797 is approximately the same size or slightly larger than BSP 1994 I 51 (Dalla Vecchia 2014: tab. 4.1.6). In the holotype of *Seazzadactylus venieri* (MFSN 21545), which is probably slightly larger than BSP 1994 I 51 (humerus in MFSN 21545 and BSP 1994 I 51 is 44 and 40 mm long, respectively; Dalla Vecchia 2019), metacarpals II and III are 18 mm long and metacarpal I is 14 mm long. Length would support the identification of metapodials A-D as metatarsals. Metapodials B, A, C and D would be metatarsals I, II, III and IV, respectively. Because of its size, also the metapodial preserved near the right tibiotarsus could be a metatarsal II or III.

Pedal/manual phalanges. Phalanges that do not belong to the wing finger and to pedal digit V are considered all together here, because of the difficulty in attributing disarticulated and scattered phalanges to the pes or manus.

Wellnhofer (2003: 8) mentioned the presence of "manual claws" in BSP 1994 I 51, but the ungual phalanx depicted in his figure 9B is identified as a "pedal claw" in the caption of the figure. I was able to identify only one ungual phalanx in BSP 1994 I 51, the one figured in Wellnhofer figure 9B, which is close to the articulated segment of the caudal vertebral column on fragment IV (Fig. 1). The ungual is partially covered proximally by the zygapophyses of a cervical vertebra; it is ventrally curved, with a deep proximal portion and a low, long, tapering and distally pointed blade (Fig. 12A). This ungual phalanx is ~6.7 mm long, measured as the distance between the distal tip of the blade and the proximal extremity. The deep proximal portion bears a well-developed flexor tubercle. The single neurovascular groove is broad and shallow and crosses the blade longitudinally. This bone resembles the pedal unguals of *Carniadactylus rosenfeldi* in its development of the proximal portion, and the proportional size and elongation of the blade (Dalla Vecchia 2014: fig. 4.1.128), but also the manual unguals of *Seazzadactylus venieri* are similar (see Dalla Vecchia 2014: fig. 21). The manual phalanges of *Eudimorphodon ranzii* (see Wild 1979: fig. 17; Dalla Vecchia 2014: fig. 4.1.92) and *Peteinosaurus zambellii* (see Wild 1979: pls. 12 and 14, fig. 38; Dalla Vecchia 2014: figs 4.1.57 and 4.1.65) have a comparatively shorter and stouter blade. As for size, the ungual of BSP 1994 I 51 is comparable to the manual phalanges of the holotype of *Seazzadactylus venieri* (6.2-7 mm long; see Dalla Vecchia 2019). The ungual phalanges of the pes of *Carniadactylus rosenfeldi* holotype, which is a slightly larger pterosaur than BSP 1994 I 51, are smaller than the ungual phalanx of BSP 1994 I 51, ranging 4.5-6 mm in length (Dalla Vecchia 2009a: tab. 1). Therefore, the skeletal element under examination is plausibly a manual ungual phalanx.

At least three non-ungual phalanges can be identified in BSP 1994 I 51 (Fig. 1). The longest non-ungual phalanx is 9 mm long and lies isolated on the lower right margin of fragment IV (in Fig. 1) near the caudal vertebrae. It is slender and elongated; its shaft tapers distally where the phalanx ends

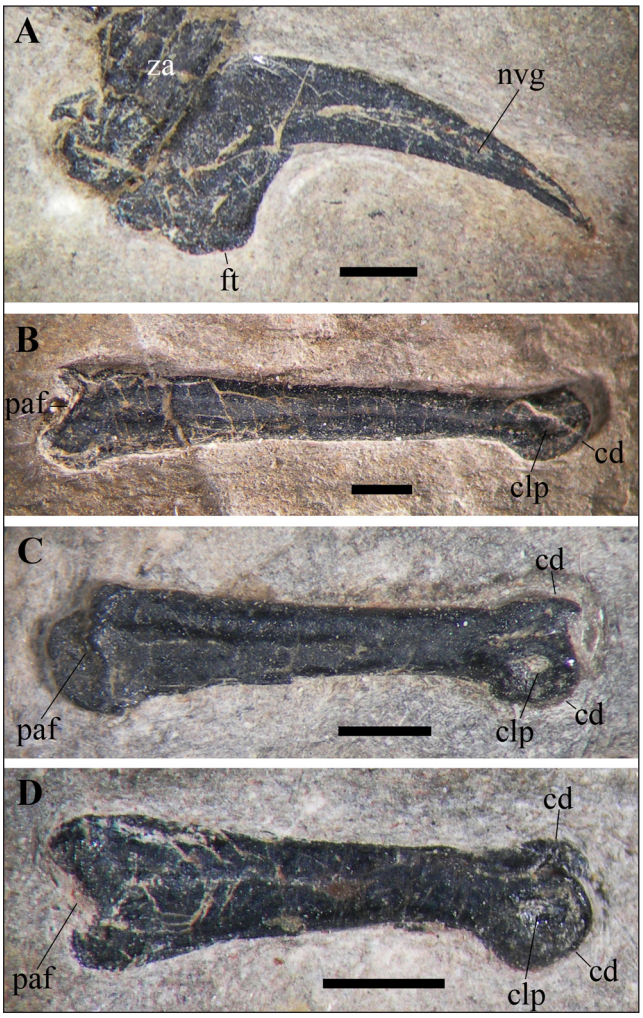

Fig. 12 - Phalanges of the holotype of *Austriadraco dallavecchiai* (BSP 1994 I 51). A) Manual ungual phalanx; B) probable penultimate phalanx from one of the digits I-III of the manus; C) elongated phalanx, possibly a proximal phalanx from one of pedal digits II-IV; and D) relatively elongated phalanx, smaller and slightly stouter than the phalanx in figure C. Abbreviations: cd, condyle; clp, pit for the collateral ligament; ft, flexor tubercle; nvg, neurovascular groove; paf, proximal articular facet; za, zygapophyses of the caudal vertebra. Scale bar equals 1 mm.

with an asymmetrical condyle (only one side of the ginglymus is exposed; Fig. 12B). The condyle shows a pit for the collateral ligament. Morphology, size and comparison with other pterosaurs suggest that this phalanx is one of the penultimate (pre-ungual) phalanges of manual digits I-III (Wild 1979: pl. 14 and figs 17-18 and 38; Dalla Vecchia 2019: fig. 21) or, less probably, a pre-ungual phalanx of pedal digit I (Wild 1979: fig. 41; Dalla Vecchia 2014: fig. 4.1.128). The asymmetrical development of the condyles allowed a high flexion of the ungual phalanx. This phalanx is not far from the only preserved ungual phalanx and is plausibly a penultimate phalanx of the manus.

The second non-ungual phalanx in terms of size is 5.8 mm long and lies isolated on fragment V (Fig. 1). It is relatively long, but it is stouter than the longest non-ungual phalanx (Fig. 12C). Its proximal expanded portion does not seem to be markedly asymmetrical in extensor view. Its shaft tapers distally where the phalanx ends with a ginglymus; both ginglymal condyles are visible because of the partial exposure of the phalanx in extensor view. The fully exposed condyle is well-shaped, with a semicircular outline and a deep pit for the collateral ligament. This phalanx resembles the comparatively elongated first phalanges of pedal digits II-IV of *Carniadactylus rosenfeldi*, which are long but more robust than the penultimate manual phalanges and pedal phalanx I-1 (Dalla Vecchia 2014: fig. 4.1.128; pers. obs.).

The last non-ungual phalanx is 4.4 mm long and is preserved on fragment IV near the caudal vertebrae and close to the longest non-ungual phalanx (Fig. 1). It is similar to the second non-ungual phalanx but it is smaller and slightly stouter (Fig. 12CD).

Discussion

Sternal plate or fused frontals?

The rhomboid bone preserved closed to the left humerus and right scapulocoracoid has been identified as a sternum by Wellnhofer (2003), but it was later referred to as the fused frontals by Bennett (2015: 801) and Kellner (2015: 674). Dalla Vecchia (2014: 88) adopted the identification as a sternum as "provisional". Wellnhofer (2003: 14) opted for the identification as a sternum because "in its general shape it agrees well with the sternum of the juvenile specimen of *E. ranzii* described by Wild (1994)". However, he was probably influenced by the close association of the one with the dorsal vertebrae and ribs, shoulder girdle elements and humeri in BSP 1994 I 51 and because of its superficial similarity to the triangular or rhomboidal sternal plates of *Dorygnathus* (see Wiman 1925: fig. 7; Padian 2008a: fig. 20).

The identification as fused frontals is plausible because of the morphological resemblance to the fused frontals of the Jurassic non-monofenestratan pterosaur *Allkaruen koi* (see Codorniú et al. 2016: fig. 1b). This explains the presence of the paired narrow processes, which would be an unusual feature in a pterosaur sternum (Wellnhofer 1978: fig. 8; Wild 1979: fig. 14; Wild 1994: fig. 6; Padian 2008a: fig. 20; Padian 2008b: fig. 12; Lü et al. 2011: fig. 4; and Dalla Vecchia 2014: fig. 4.2.2). Bennett (2015: 801) identified those processes as the lacrimal processes of the frontals. In some non-monofenestratan pterosaurs, the lacrimal probably does not reach the frontal but the nasal does (e.g. *E. ranzii*, Wild 1979: fig. 1; *Campylognathoides liasicus*, Wellnhofer 1974: fig. 3 and Padian 2008b: figs 4, 6 and 10; *Dorygnathus banthensis*, Padian 2008b: figs 16 and 18; *Parapsicephalus purdoni*, O'Sullivan & Martill 2017; fig. 5; *Rhamphorhynchus muensteri*, Wellnhofer 1975a: fig. 3a-b and 1975b: figs 26-27). In any case, the lacrimal would articulate with the rostral process of the frontal laterally, if it reached it. The rostral projection of the process suggests a contact with a corresponding posterior process of the nasal, as it seems the case with the pterosaurs listed above. Codorniú et al. (2016: fig. 1b) identified the rostral processes of the frontals of *Allkaruen* as the nasal processes. Therefore, I consider provisionally the rostral processes of the frontals as the nasal processes.

Besides the long rostral processes, some other unusual features have made the identification of the skeletal element of BSP 1994 I 51 as the fused frontals not immediate.

In dorsal and ventral view, the fused frontals have concave lateral margins, because they form the upper margin of the orbits (e.g. Wellnhofer 1974: fig. 2; Wild 1979: fig. 1 and pl. 3a; Padian 2008a: fig. 13, 2008b: figs 4, 6, pl. 6/fig. 2, and pl. 7/fig. 2; Hone et al. 2013: fig. 9C; Bennett 2014: fig. 2; Zhou 2014: fig. 2; Codorniú et al. 2016: fig. 1b; Fig. 13), whereas they are slightly convex for most of the lateral margin in BSP 1994 I 51 and become concave only in correspondence with the rostral processes (Fig. 5A-D). This unexpected outline of the orbital margin may be a consequence of the crushing and flattening of the bone, or the arched margin of the orbit was partly formed by another circumorbital element (i.e. the supraorbital). Also the orbital margin of the right frontal (the orbital margin of the left frontal is damaged) of the holotype of *Eudimorphodon ranzii* does not look like the frontal would border the orbit (see Fig. 13).

No pointed process divides longitudinally the rostral median notch for the dorsocaudal processes of the premaxillae in pterosaur frontals (e.g. Wild 1979: fig. 1a; Padian 2008b: pl. 7/fig. 2; Andres et

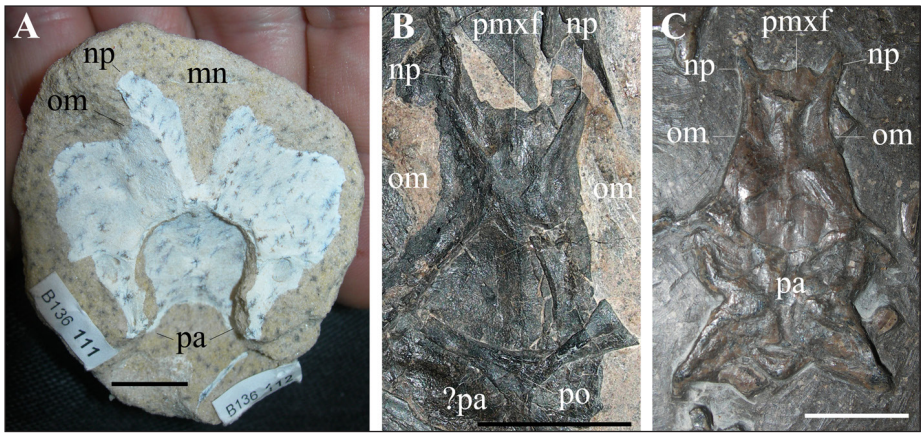

Fig. 13 - Frontoparietals of some basal non-monofenestratan pterosaurs. A) Holotype of *Caelestiventus hanseni*, BYU 20707, ventral view; B) holotype of *Eudimorphodon ranzii*, MCSNB 2888, dorsal view; C) *Campylognathoides liasicus*, SMNS 50735, dorsal view. Abbreviations: mn, median notch; np, nasal process; om, orbital margin; pa, parietals; pmxf, facet for the dorsocaudal processes of the premaxillae; po, postorbital. The scale bars equal 10 mm.

al. 2010; fig. 4A; Dalla Vecchia 2014: fig. 4.1.82; Codorniú et al. 2016: fig. 1b; Britt et al. 2018: fig. 3n-o; Fig. 13B). This appears to be an autapomorphy of *Austriadraco dallavecchiai*, although the process may be present but broken in the frontals of *Allkaruen koi* (see Codorniú et al. 2016: fig. 1b) and the condition is unknown in many Triassic pterosaurs in which the frontals are poorly preserved or not preserved at all (i.e. *Preondactylus buffarinii*, *Austriadactylus cristatus*, *Arcticodactylus cromptonellus*, *Seazzadactylus venieri*, *Carniadactylus rosenfeldi*, MCSNB 8950, *Caviramus schesaplanensis*, *'Raeticodactylus' filisurensis*, and *Peteinosaurus zambellii*).

The fused frontals are not closely associated with skull bones, in particular with the cluster containing postorbital, squamosal, supraorbital or parietal, and sclerotic ring elements; conversely, they are associated with the elements that surround the sternum in the articulated skeleton (Fig. 1). However, the skeleton is disarticulated and skeletal elements and clusters of elements have prevalently drifted in the lower right direction (according to the orientation of the block in Fig. 1), as indicated by the distribution of most of the preserved elements. This drift was probably caused by weak currents at the bottom of the stagnant and anoxic basin on the macerated and decaying carcass. The broad and relatively flat frontal plate plausibly had a different behaviour to the hydrodynamic stresses compared to the other skull elements with a different morphology. Although the frontal plate clusters with axial and limb bones, it is in the drifting trajectory of the other skull bones and not far from them.

Finally, the sutural line between the two frontals could be mistaken for the thin ventral keel of the sternum of early pterosaurs (Wellnhofer 1975a: fig. 8d; Wild 1979: fig. 14; Dalla Vecchia 2014: fig. 4.2.2A-B). The presence of the suture and the lack of fusion between frontals and parietals is a further evidence of immaturity of BSP 1994 I 51, which adds to the unobliterated suture between the premaxillae and the overall disarticulation of the skull.

Diagnostic features of *Austriadraco dallavecchiai*

A comparison between *Austriadraco dallavecchiai* and closely related non-monofenestratan pterosaurs shows that most of the five autapomorphies and the apomorphic combination of characters within non-pterodactyloid pterosaurs listed by Kellner (2015) for this taxon are not apomorphic or at least they are ambiguous or they are incorrectly formulated.

Apomorphy 1: "Frontal with short anterior processes". The nasal processes are not comparatively shorter than in other pterosaurs, but they are rather thinner (Fig. 13). *Allkaruen koi* has (see Codorniú et al. 2016: fig. 1b) similar nasal processes, but they are much shorter than those of BSP 1994 I 51, if they are complete. The feature that is unique to the fused frontals of *Austriadraco dallavecchiai* is the rostromedian process (Fig. 5), which is absent in the frontals of other pterosaurs (Fig. 13; see discussion and references above). In the amended diagnosis, I reformulate the diagnostic feature of Kellner (2015) as "large frontals with very narrow and long rostral (nasal) processes and a shorter and pointed rostromedian process in the plate originated from their fusion". However, this is an ambiguous diagnostic feature because the frontals are unknown in *Seazzadactylus venieri* and poorly preserved in *Carniadactylus rosenfeldi*, which are closely related to *Austriadraco dallavecchiai* (see Dalla Vecchia 2019).

Apomorphy 2: "Jugal with small maxillary and nasal processes, and a thin and elongated postorbital process". A "thin and elongated" postorbital process is shared with *Seazzadactylus venieri* (see Dalla Vecchia 2019: fig. 7), thus the shape and size of this process is not apomorphic of the Austrian taxon. The maxillary (rostroventral) and "nasal" (actually, rostrodorsal or lacrimal because it contacts the lacrimal in early pterosaurs) processes are not only small (they are small also in other pterosaurs, e.g. *Campylognathoides liasicus*, see Wellnhofer 2003: fig. 3C), but they are both rostrally directed forming an angle of only 11° in a way that the ventrocaudal end of the antorbital fenestra had to be very narrow. Therefore, the definition of this diagnostic character has been reformulated.

Apomorphy 3: "Presence of an external mandibular fenestra". This is a plesiomorphic feature for the Archosauriformes (e.g. Nesbitt 2011; Bennett 2015) or *Tasmaniosaurus triassicus* + Archosauriformes (Ezcurra 2016), but it is not found in any other pterosaur (Bennett 2015), including *Seazzadactylus venieri* (see Dalla Vecchia 2019), thus it can be considered as an autapomorphy of *Austriadraco dallavecchiai*.

Apomorphy 4: "Surangular dorsal process low". This process has the same morphology in *Seazzadactylus venieri* (see Dalla Vecchia 2019: fig. 10), thus it is not an apomorphy of *Austriadraco dallavecchiai*. Furthermore, the surangular process is "low" in most other pterosaurs (Wellnhofer 1978; Dalla Vecchia 2014).

Apomorphy 5: "Scapula significantly longer than the coracoid (sc/co ~ 1.62)". The state of this character is unknown in some taxa that are phylogenetically close to *Austriadraco dallavecchiai*, namely *Seazzadactylus venieri*, *Carniadactylus rosenfeldi* and *'Raeticodactylus' filisurensis* (see Dalla Vecchia 2019). The scapulocoracoid is not preserved in the only specimen of *'Raeticodactylus' filisurensis* (see Stecher 2008), whereas the scapula is incompletely preserved in *Seazzadactylus venieri* and *Carniadactylus rosenfeldi* (see Dalla Vecchia 2019). However, the coracoids of *Seazzadactylus venieri* and *Carniadactylus rosenfeldi* have broad and flat shafts like that of *Austriadraco dallavecchiai* and unlike those of most other non-monofenestratan pterosaurs, which are rod-like (e.g. *Eudimorphodon ranzii*, see Wild 1979: fig. 15; *Campylognathoides liasicus*, see Wellnhofer 1974: fig. 6; *Rhamphorhynchus muensteri*, see Wellnhofer 1975a: fig. 9). This similarity of the coracoids in the three Triassic taxa may be generalized to the proportions of the entire scapulocoracoids; thus considering "scapula significantly longer than the coracoid" an apomorphy of *Austriadraco dallavecchiai* alone is risky. In fact, the scapula is also "significantly" longer than the coracoid in other three Triassic pterosaur specimens: the holotype of *Arcticodactylus cromptonellus* (MGUH VP 3393; see Jenkins et al. 2001: fig. 2; ratio sc/co ~ 2), MCSNB 8950 (see Wild 1994: fig. 2; ratio sc/co ~ 2) and MCSNB 2887 (see Wild 1979: fig. 16; ratio sc/co ~ 1.55). *Arcticodactylus cromptonellus* and MCSNB 8950 belong to the same clade as *Austriadraco dallavecchiai*, *Seazzadactylus venieri*, *Carniadactylus rosenfeldi* and *'Raeticodactylus' filisurensis* (see Dalla Vecchia 2019).

The apomorphic combination of characters of Kellner (2015) is "broad coracoid with constricted shaft; deep ischiopubic plate; comparatively long tibia relative to the humerus (humerus/tibiotarsus length < 0.70) and to the wing phalanx 1 (wing phalanx 1/tibiotarsus length - 0.92)". It is unclear to this author where the shaft of the coracoid is constricted in *Austriadraco dallavecchiai*. The shaft of the coracoid is fan-shaped in BSP 1994 I 51, with distally diverging margins and is much broader distally than proximally (Wellnhofer 2013: fig. 12A, Dalla Vecchia 2014: fig. 4.1.40). This is a diagnostic feature of *Austriadraco dallavecchiai*, because the broad coracoid shafts of *Carniadactylus rosenfeldi* (see Dalla Vecchia 2009a: fig. 3C-D) and *Seazzadactylus venieri* (see Dalla Vecchia 2019: fig. 18) have nearly parallel margins. Also the coracoid of *Arcticodactylus cromptonellus* is not fan-shaped (Jenkins et al. 2001: fig. 2).

Kellner (2015: 677) affirms that the pelvis of BSP 1994 I 51 is "much deeper than in *Eudimorphodon ranzii*", but the pelvis is poorly preserved in the holotype and the only specimen of the latter taxon (MCSNB 2888); the only preserved pelvic plate is strongly crushed and misshapen and probably incomplete (Wild 1979: pl. 2; Dalla Vecchia 2014: fig. 4.1.87), thus comparison is impossible. The ischiopubic plate is relatively deep in all pterosaurs (e.g. *Peteinosaurus zambellii*, see Wild 1979: figs 19; Dalla Vecchia 2014: figs 4.1.58 and 72; *Carniadactylus*

rosenfeldi, see Dalla Vecchia 2014: figs 4.1.123A-B; MCSNB 8950, Wild 1993: fig. 5; *Dimorphodon macronyx*, see Sangster 2003: figs 3.15, 5.10, 5.12-13 and 5.35; *Dorygnathus banthensis*, see Wiman 1925: fig. 8; Padian 2008b: figs14 and 21; *Rhamphorhynchus muensteri*, see Wellnhofer 1975a: fig. 10a, d and g). Thus, the depth of this plate must be quantified. Its height/length ratio, with height measured from the ventral margin of the acetabulum to the ventralmost point of the plate, is 0.55, 0.54-0.63, 0.66-0.71 and 0.66 in *Peteinosaurus zambellii*, *Dimorphodon macronyx*, *Dorygnathus banthensis*, and *Rhamphorhynchus muensteri*, respectively. The height of the ischiopubic plate of BSP 1994 I 51 measured as reported at p. 438 coincides with that based on the position of the acetabulum as reconstructed by Wellnhofer (2003). Therefore, the ratio of BSP 1994 I 51 (0.85) is higher than that of the pterosaurs listed above, but this is a consequence of the craniocaudally short caudal process of the ischium. Furthermore, the relative depth of the ischiopubic plate of the taxa closer to *Austriadraco dallavecchiai* (i.e. *Arcticodactylus cromptonellus*, *Seazzadactylus venieri*, *Carniadactylus rosenfeldi*, *Caviramus schesaplanensis* and *'Raeticodactylus' filisurensis*) is unknown.

The shape of the caudal process of the ischium appears to be more taxonomically informative than a slightly deeper ischiopubic plate. This process has a sub-rectangular outline in lateral view (Fig. 13B), being more similar to those sub-trapezoidal of *Peteinosaurus zambellii* (see Dalla Vecchia 2014: figs 4.1.67 and 72), *Austriadactylus cristatus* (see Dalla Vecchia 2014: fig. 4.1.21), and possibly *Preondactylus buffarinii* (see Dalla Vecchia 2014: figs 4.1.2 and 7) than those of *Dimorphodon macronyx* (see Sangster 2003: figs 3.15, 5.10, 5.12-13 and 5.35), *Dorygnathus banthensis* (see Arthaber 1921: fig. 44; Wiman 1925: fig. 8; Padian 2008b: fig. 21), *Rhamphorhynchus muensteri* (see Wellnhofer 1975a: fig. 10a, d and g), *Darwinopterus linglontaensis* (see Wang et al. 2010: fig. 5b), and *Darwinopterus robustodens* (see Lü et al. 2011: fig. 5i). However, the caudal process of the ischium of *Austriadraco dallavecchiai* does not taper distally like those of *Preondactylus buffarinii* and *Austriadactylus cristatus* and is proportionally much deeper (it is higher than long). Considering the caudal process as beginning at level of the small dorsocaudal process of ischium, the ratio between the height of the distal side of the process and the length of the process is 1.40 in *Austriadraco dallavecchiai* and 0.42 in *Peteinosaurus zambellii* (MCSNB 3496). The ratio between the height of the distal side of the caudal process and the total height of the ischium is 0.28 in *Peteinosaurus zambellii* (MCSNB 3496) and 0.71 in *Austriadraco dallavecchiai*.

The pelvis of *Seazzadactylus venieri* is incompletely preserved; the height/length ratio of the ischiopubic plate cannot be calculated. However, the caudal process of ischium is completely preserved and, unlike the statement by Dalla Vecchia (2019: 38), is different from that of *Austriadraco dallavecchiai* (see Fig. 14).

Furthermore, the ischium of *Austriadraco dallavecchiai* has a cranioventral triangular process that is unreported in other pterosaurs. Therefore, "rectangular and deeper than long caudal process of ischium with the height of its distal side that is over 70% the total height of the ischium; and ischium bearing a large and ventrally directed triangular process in the ventral margin" are considered diagnostic features of *Austriadraco dallavecchiai*, to be confirmed with the discovery of further specimens of *Arcticodactylus cromptonellus*, *Seazzadactylus venieri*, *Carniadactylus rosenfeldi*, *Caviramus schesaplanensis* and *'Raeticodactylus' filisurensis* that preserve the ischiopubic plate.

In BSP 1994 I 51, the humerus/tibiotarsus and wing phalanx 1/tibiotarsus length ratios are 0.69 and 0.92, respectively. They are 0.73 and 0.81 in *Preondactylus buffarinii,* 0.88 and 0.89 in *Arcticodactylus cromptonellus* (obtained from the length of the tibia only, because proximal tarsals are unfused to the tibia in the immature single specimen of this species), 0.77 and 1.18 in *Carniadactylus rosenfeldi*, 1.04 and1.36 in MCSN 8950, 0.98 and 1.34 in *'Raeticodactylus'filisurensis*, 0.81 and 0.82-0.88 in *Peteinosaurus zambellii*, and 0.70-0.75 and 0.80-0.85 in *Dimorphodon macronyx* (see Dalla Vecchia 2014, 2019 and Sangster 2003). The humerus/tibiotarsus and wing phalanx 1/tibiotarsus length ratios in *Seazzadactylus venieri* are 0.96/1.00 and 1.1, respectively, but are based on approximate or estimated measurements of humerus and tibiotarsus.

Apparently, values of BSP 1994 I 51 ratios are distinct from those of the other Triassic pterosaurs and *Dimorphodon macronyx*. However, these ratios are based on single specimens, with the sole exception of *Peteinosaurus zambellii* (two specimens) and *Dimorphodon macronyx* (three specimens). If the intraspecific ranges of these ratios are analyzed in a larger sample, it is evident that the difference be-

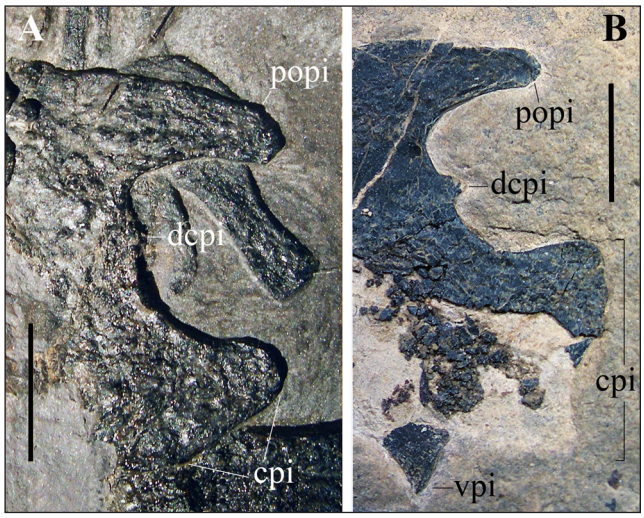

Fig. 14 - Caudal portion of the pelvic plate of *Seazzadactylus venieri* and *Austriadraco dallavecchiai*. A) *Seazzadactylus* venieri, holotype (MFSN 21545); B) *Austriadraco dallavecchiai*, holotype (BSP 1994 I 51). Abbreviations: cpi, caudal process of ischium; dcpi, dorsocaudal process of ischium; popi, postacetabular process of ilium; vpi, ventral process of ischium. The scale bars equal 5 mm.

tween the values of BSP 1994 I 51 ratios and those of the other pterosaurs can be due to sampling. The largest available sample of a single pterosaur species is that of *Rhamphorhynchus muensteri* (see Wellnhofer 1975b; Supplementary Information). According to Bennett (1995), this sample includes three size-classes representing three distinct growth stages of a single species. In this sample, the humerus/tibia (tibiotarsus) length ratios range 0.76-1.20 and there is a high variability also within the two main size classes (SI Fig.1A). Worthy of note is that the tibia (tibiotarsus) is shorter than the humerus in some of the small specimens and in one of the largest specimens, while it is longer in the medium-size class (SI Fig. 1A). The values distribution of humerus/tibia (tibiotarsus) ratios reflects the allometric growth of the two skeletal elements, with a decrease of the ratio with the increase of body size in the small and medium-size classes and an increase in the few specimens belonging to the large-size class. These changes with increase of body size are related to the increase of relative length of the tibia due to the fusion of astragalus and calcaneum during ontogeny (see Supplementary Information) as well as the negative allometric growth of the humerus, as suggested by the absence of a marked decrease of the wing phalanx 1/tibiotarsus ratio with the increase of body size.

The wing phalanx 1/tibia (tibiotarsus) length ratios of *R. muensteri* range 2.08-2.68. The high ratio variability is similar within the two main size classes and is even higher than for the humerus/tibia (tibiotarsus) length ratio (SI Fig.1B).

The second largest available sample of a single non-monofenestratan pterosaur species is that of *Dorygnathus banthensis* (see Padian 2008a: tab. 1). In this sample, the humerus/tibia (tibiotarsus) length ratios range 0.65-1.07 and the wing phalanx1/tibia (tibiotarsus) length ratios range 0.81-1.27 (see Supplementary Information). There is no trend within the ratios with wing span increase (SI Fig. 2).

This high intraspecific variability of humerus/tibiotarsus and wing phalanx 1/tibiotarsus length ratios within a single species suggests being careful in using ratios for taxonomic purposes, especially when their intraspecific range is unknown.

The holotype of *Austriadraco dallavecchiai* also shows some unique features in the dentition. Multicusped tooth crowns bear a 'parasite' cuspule on the larger accessory cusps, which is unreported in other Triassic pterosaurs (Dalla Vecchia 2014, 2019). The presence of the 'parasite' cuspule appears to be occasional in the multicusped mandibular teeth, but this cuspule is very small and is clearly visible only in the SEM photograph of the tooth (see Wellnhofer 2003: fig. 8). 'Parasite' cuspules are instead evident in the isolated maxillary tooth.

A mandibular tooth 3 with distally recurved crown bearing small cuspules at the base of the mesial margin and along most of the distal margin is not reported in any other pterosaur (Wellnhofer 1978; Dalla Vecchia 2014), although the mandibular tooth 3 of *Seazzadactylus venieri* has some small cusps along the cutting margins (see below).

Austriadraco dallavecchiai and *Seazzadactylus venieri*

Dalla Vecchia (2019) underlined the close relationships between *Austriadraco dallavecchiai* and *Seazzadactylus venieri*, which was also supported by his phylogenetic analysis, although the two did not turn out to be sister taxa (Dalla Vecchia 2019: fig. 24). They are sister taxa in the analysis by Ezcurra et al. (2020: fig. 3) which, however, does not include all pterosaur taxa and all the characters of the analysis by Dalla Vecchia (2019). Unlike Dalla Vecchia's (2019), the phylogenetic analysis by Ezcurra et al. (2020) was not focused on disentangling the phylogenetic relationships of earliest pterosaurs.

The present work finds further support for the close relationships between *Austriadraco dallavecchiai* and *Seazzadactylus venieri*. These two taxa share several features, including a slender and long caudodorsal (postorbital) process of the jugal (Dalla Vecchia 2010: fig. 6B-C and 7C), which could be unique to these two taxa; a triradiate postorbital, with very slender processes (Dalla Vecchia 2018: fig. 3A-B, 2019: fig. 6A); the same shape of the dorsal margin of the mandible from the last mandibular tooth to the cotyle for the quadrate, including the dorsal process of the surangular ('coronoid' process) (Dalla Vecchia 2019: fig. 10), which is unique to these two taxa; similar-shaped crowns of premaxillary teeth, with apicobasal ridges (Wellnhofer 2003: fig. 4B; Dalla Vecchia 2014: fig. 4.1.36A, 2019: fig. 11); multicusped mandibular and maxillary teeth with smooth crowns (Wellnhofer 2003: figs 5-8; Dalla Vecchia 2019: figs 12-15); a third mandibular tooth with several small accessory cusps (Fig. 7D-E); a broad and plate-like shaft of the coracoid (Wellnhofer 2003: fig. 12; Dalla Vecchia 2014: fig. 4.1.40, 2019: fig. 18); similar manual ungual phalanges (Fig. 12A; Dalla Vecchia 2019: fig. 21); and wing phalanx 3 longer than wing phalanx 1. The scapular blade flares distally in both taxa, although that of *S. venieri* is already broad proximally (Wellnhofer 2003: fig. 12; Dalla Vecchia 2014: fig. 4.1.40, 2019: fig. 18); *A. dallavecchiai* has a rounded distal termination of the scapular blade which might be apomorphic (Dalla Vecchia 2014: 82); as the scapulae of *S. venieri* flare distally, their distal ends may also be rounded, but they are not preserved in the only specimen of this species, thus a complete scapula of the Italian taxon is needed to decide whether or not a rounded termination of the scapula is synapomorphic of the two taxa.

However, *Seazzadactylus venieri* is distinct from *Austriadraco dallavecchiai*. It has a differently shaped jugal (except the long postorbital process) and a differently shaped caudoventral end of the antorbital fenestra (Dalla Vecchia 2019: figs 6B-C-7); the jugal ramus of the postorbital seems to overlap the postorbital ramus of the jugal cranially in *S. venieri* and caudally in *A. dallavecchiai* (Dalla Vecchia 2019: fig. 7). *S. venieri* lacks an external mandibular fenestra (Dalla Vecchia 2019: fig. 10); the crown of mandibular tooth 3 is not recurved distally and has small accessory cusps only in the basal tract of the mesial and distal cutting margins (Fig. 7D-E); in general, the cusp formula of mandibular teeth is different in the two taxa (Dalla Vecchia 2019: fig. 14); the multicusped teeth of *S. venieri* lack 'parasite' cuspules on the larger accessory cusps (Dalla Vecchia 2019: figs 12B-I and 15C-H); the shaft of its coracoid is not expanded distally and fan-shaped and the scapular blade is already broad proximally; and the caudal process of the ischium has a different shape in the two taxa (Fig. 14). Although incompletely preserved and with the caution suggested above, the tibiotarsus of *S. venieri* is comparatively shorter than that of *A. dallavecchiai* (it is shorter than the wing phalanx 1).

Conclusions

The study of BSP 1994 I 51 allowed the description of skeletal elements that had not been previously identified or described by Wellnhofer (2003) and Kellner (2015): the premaxillae with two associated teeth, fragments of the maxillae and two maxillary teeth, a purported supraorbital or partial parietal, a postorbital, a possible squamosal, elements of the sclerotic ring, the basisphenoid with the basipterygoid processes, a possible ulna, a proximal syncarpal, at least two phalanges of manual digits I-III, the left wing phalanx 1, the right wing phalanges 2-4, the left femur and tibiotarsus, a medial distal tarsal and several metapodials (the better preserved ones are probably metatarsals).

The identification as the fused frontals of the bone previously referred to the sternum by Wellnhofer (2003), proposed by Bennett (2015) and Kellner (2015), is confirmed.

A revised diagnosis of *Austriadraco dallavecchiai* has been possible based on these previously undescribed elements and by comparison to the closely related *Seazzadactylus venieri*. *Austriadraco dallavecchiai* has a peculiar jugal, frontals, shaft of the coracoid and ischium, an external mandibular fenestra, multicusped tooth crowns with a 'parasite' cuspule on the larger accessory cusps, and a mandibular tooth 3 with distally recurved crown bearing cuspules along the cutting margins.

Austriadraco dallavecchiai and *Seazzadactylus venieri* share several skeletal features (including the thin and long postorbital process of the jugal and the shape of the dorsal process of the surangular, which had been considered apomorphies of *Austriadraco dallavecchiai* by Kellner 2015), but are clearly distinct taxa.

Acknowledgements: I thank O. Rauhut for access to the specimen at BSP. I am indebted to the reviewers David Martill and Kevin Padian for their valuable comments and suggestions.

References

Andres B., Clark J. M. & Xing X. (2010) - A new rhamphorhynchid pterosaur from the Upper Jurassic of Xinjiang, China, and the phylogenetic relationships of basal pterosaurs. *Journal of Vertebrate Paleontology*, 30(1): 163-187.

Arthaber G., von (1921) - Studien über Flugsaurier auf grund der Bearbeitung des wiener Exemplares von *Dorygnathus banthensis* Theod. sp.. *Denkschriften der Akademie der Wissenschaften Wien, Mathematisch-naturwissenschaftliche Klasse*, 97: 391-464.

Barrett P.M., Butler R.J., Edwards N.P. & Milner A.R. (2008) - Pterosaur distribution in time and space: an atlas. *Zitteliana*, B28: 61-107.

Bennett S.C. (1995) - A statistical study of *Rhamphorhynchus* from the Solnhofen Limestone of Germany: year-classes of a single large species. *Journal of Paleontology*, 69: 569-580.

Bennett S.C. (2001) - The osteology and functional morphology of the Late Cretaceous pterosaur *Pteranodon*. *Palaeontographica Abt A*., 260: 1-153.

Bennett S.C. (2014) - A new specimen of the pterosaur *Scaphognathus crassirostris*, with comments on constraint of cervical vertebrae number in pterosaurs. *Neue Jahrbuch für Geologie und Paläontologie Abhandlungen*, 271(3): 327-348.

Bennett S.C. (2015) - An external mandibular fenestra and other archosauriform characters in basal pterosaurs reexamined. *Historical Biology*, 27: 796-814.

Britt B.B., Dalla Vecchia F.M., Chure D.J., Engelmann G.F., Whiting M.F. & Scheetz R.D. (2018) - *Caelestiventus hanseni* gen. et sp. nov. extends the desert-dwelling pterosaur record back 65 million years. *Nature Ecology & Evolution*, 2(9):1386-1392.

Butler R.J., Barrett P.M. & Gower D.J. (2009) - Postcranial skeletal pneumaticity and air-sacs in the earliest pterosaurs. *Biological Letters*, 5: 557-560.

Codorniú L., Paulina-Carabajal A., Pol D., Unwin D.M. & Rauhut O.W.M. (2016) - A Jurassic pterosaur from Patagonia and the origin of the pterodactyloid neurocranium. *PeerJ* 4: e2311; doi 10.7717/peerj.2311.

Dalla Vecchia F.M. (2002) - A caudal segment of a Late Triassic pterosaur (Diapsida, Pterosauria) from Northeastern Italy. *Gortania - Atti Museo Friulano di storia Naturale,* 3(2001): 31-58.

Dalla Vecchia F. M. (2003) - New morphological observations on Triassic pterosaurs. In: Buffetaut E., Mazin J.-M. (Eds.) - Evolution and palaeobiology of pterosaurs. *Geological Society London, Special Publications*, 217: 23-44.

Dalla Vecchia F.M. (2004a) - An *Eudimorphodon* (Diapsida, Pterosauria) specimen from the Norian (Late Triassic) of north-eastern Italy. *Gortania - Atti Museo Friulano di Storia Naturale*, 25(2003): 47-72.

Dalla Vecchia F.M. (2004b) - A review of the Triassic pterosaur record. *Rivista del Museo Civico di Scienze Naturali "E. Caffi" Bergamo*, 22 (2003): 13-29.

Dalla Vecchia F.M. (2006) - The tetrapod fossil record from the Norian-Rhaetian of Friuli (northeastern Italy). In: Harris J., Lucas S.G., Spielmann J.A., Lockley M.G., Milner A.R.C. & Kirkland J.I. (eds) - The Triassic-Jurassic Terrestrial Transition. *New Mexico Museum of Natural History and Science Bulletin*, 37: 432-444.

Dalla Vecchia F.M. (2009a) - Anatomy and systematics of the pterosaur *Carniadactylus* gen. n. *rosenfeldi* (Dalla Vecchia, 1995). *Rivista Italiana di Paleontologia e Stratigrafia*, 115: 159-186.

Dalla Vecchia F.M. (2009b) - *Austriadactylus* (Diapsida, Pterosauria) from the Norian (Upper Triassic) of northeastern Italy. *Rivista Italiana di Paleontologia e Stratigrafia*, 115: 291-304.

Dalla Vecchia F.M. (2013) - Triassic pterosaurs. In: Nesbitt S.J., Desojo J.B., Irmis R.B. (Eds) -Anatomy, Phylogeny and Palaeobiology of Early Archosaurs and their Kin. *Geological Society London, Special Publications,* 379: 119-155.

Dalla Vecchia F.M. (2014) - Gli pterosauri triassici. Pubblicazione del Museo Friulano di Storia Naturale n. 54, Museo Friulano di Storia Naturale, Udine, 319 pp.

Dalla Vecchia F.M. (2018) - Comments on Triassic pterosaurs with a commentary on the "ontogenetic stages" of Kellner (2015) and the validity of *Bergamodactylus wildi*. *Rivista Italiana di Paleontologia e Stratigrafia*, 124(2): 317-341.

Dalla Vecchia F.M. (2019) - *Seazzadactylus venieri* gen. et sp. nov., a new pterosaur (Diapsida: Pterosauria) from the Upper Triassic (Norian) of northeastern Italy. *PeerJ*, 7: e7363; doi 10.7717/peerj.7363

Dalla Vecchia F.M., Wild R., Hopf H. & Reitner J.A. (2002) - A crested rhamphorhynchoid pterosaur from the Late Triassic of Austria. *Journal of Vertebrate Paleontology*, 22: 195-198.

Ezcurra M.D. (2016) - The phylogenetic relationships of basal archosauromorphs, with an emphasis on the systematics of proterosuchian archosauriforms. *PeerJ*, 4: e1778; doi 10.7717/peerj.1778

Ezcurra M.D., Nesbitt S.J., Bronzati M., Dalla Vecchia F.M., Agnolin F.L., Benson R.B.J., Brissón Egli F., Cabreira S.F., Evers S.W., Gentil A.R., Irmis R.B., Martinelli A.G., Novas F.E., Roberto-da Silva L., Smith N.D., Stocker M.R., Turner A.H. & Langer M.C. (2020) - Enigmatic dinosaur precursors bridge the gap to the origin of Pterosauria. *Nature*, 588: 445-449.

Fröbisch N.B. & Fröbisch J. (2006) - A new basal pterosaur genus from the Upper Triassic of Northern Calcareous Alps of Switzerland. *Palaeontology*, 49: 1081-1090.

Hyder E.S., Witton M.P. & Martill D.A. (2014) - Evolution of the pterosaur pelvis. *Acta Palaeontologica Polonica*, 59(1): 109-124.

Jenkins F.A. Jr., Shubin N.H., Gatesy S.M. & Padian K. (2001) - A diminutive pterosaur (Pterosauria: Eudimorphodontidae) from the Greenlandic Triassic. *Bulletin of the Museum of Comparative Zoology*, 156: 151-170.

Kaup J.J. (1834) - Versuch einer Eintheilung der Saugethiere

in 6 Stämme und der Amphibien in 6 Ordnungen. *Isis*, 3: 311-315.

Kellner A.W.A. (2003) - Pterosaur phylogeny and comments on the evolutionary history of the group. In: Buffetaut E., Mazin J.-M. (Eds.) - Evolution and palaeobiology of pterosaurs. *Geological Society London, Special Publications,* 217: 105-137.

Kellner A.W.A. (2015) - Comments on Triassic pterosaurs with discussion about ontogeny and description of new taxa. *Anais Academia Brasileira de Ciências*, 87(2): 669-689.

Lü J., Xu L., Chang H. & Zhang X. (2011) - A new darwinopterid pterosaur from the Middle Jurassic of Western Liaoning, northeastern China and its ecological implications. *Acta Geologica Sinica*, 85: 507-514.

Nesbitt S.J. (2011) - The early evolution of Archosauria: relationships and the origin of major clades. *Bulletin of the American Museum of Natural History*, 352: 1-292.

Nesbitt S.J. & Hone D.W.E. (2010) - An external mandibular fenestra and other archosauriform character states in basal pterosaurs. *Palaeodiversity*, 3: 225-233.

Osborn H.F. (1903) - On the primary division of the Reptilia into two sub-classes, Synapsida and Diapsida. *Science*, 17(424): 275-276.

Ősi A. (2010) - Feeding-related characters in basal pterosaurs: implications for jaw mechanism, dental function and diet. *Lethaia*, 44(2): 136-152

Padian K. (1980) - Note on a new specimen of pterosaur (Reptilia. Pterosauria) from the Norian (Upper Triassic) of Endenna, Italy. *Rivista del Museo Civico di Scienze Naturali "E. Caffi" Bergamo*, 2: 119-127.

Padian K. (1983) - Osteology and functional morphology of *Dimorphodon macronyx* (Buckland) (Pterosauria. Rhamphorhynchoidea) based on new material in the Yale Peabody Museum. *Postilla*, 189: 1-43.

Padian K. (2008a) - The Early Jurassic pterosaur *Dorygnathus banthensis* (Theodori, 1830). *Special Papers in Palaeontology*, 80: 1-64.

Padian K. (2008b) - The Early Jurassic pterosaur *Campylognathoides* Strand, 1928. *Special Papers in Palaeontology*, 80: 65-107.

Romer A. S. (1956). Osteology of Reptiles. University of Chicago Press, Chicago, 3rd edition (1976), 772 pp.

Sangster S. (2003) - The anatomy, functional morphology and systematics of *Dimorphodon macronyx* (Diapsida: Pterosauria). PhD thesis, University of Cambridge, Cambridge (UK).

Stecher R. (2008) - A new Triassic pterosaur from Switzerland (Central Australpine, Grisons), *Raeticodactylus filisurensis* gen. et sp. nov. *Swiss Journal of Geosciences*, 101: 185-201.

O'Sullivan M. & Martill D. M. (2017) - The taxonomy and systematics of *Parapsicephalus purdoni* (Reptilia: Pterosauria) from the Lower Jurassic Whitby Mudstone Formation, Whitby, U.K. *Historical Biology*, 29: 1009-1018.

Unwin D.M. (2003) - On the phylogeny and evolutionary history of pterosaurs. In: Buffetaut E. & Mazin J.-M. (Eds) - Evolution and Palaeobiology of Pterosaurs. *Geological Society of London, Special Publications*, 217: 139-190.

Unwin D.M. (2004) - *Eudimorphodon* and the early history of pterosaurs. *Rivista del Museo Civico di Scienze Naturali "E. Caffi" Bergamo*, 22: 39-46.

Wang X., Kellner A.W.A., Jiang S., Cheng X., Meng X. & Rodrigues T. (2010) - New long-tailed pterosaurs (Wukongopteridae) from western Liaoning, China. *Anais da Academia Brasileira de Ciências*, 82: 1045-1062.

Wellnhofer P. (1974) - *Campylognathoides liasicus* (Quenstedt), an Upper Liassic pterosaur from Holzmaden. The Pittsburgh Specimen. *Annales of the Carnegie Museum*, 45(2): 5-34.

Wellnhofer P. (1975a) - Die Rhamphorhynchoidea (Pterosauria) der Oberjura-Plattenkalke Süddeutschlands. Teil I: Allgemaine Skelettmorphologie. *Palaeontographica*, 148: 1-33.

Wellnhofer P. (1975b) - Die Rhamphorhynchoidea (Pterosauria) der Oberjura-Plattenkalke Süddeutschlands. Teil II: Systematische Beschereibung. *Palaeontographica*, 148: 132-186.

Wellnhofer P. (1978) - Pterosauria. Handbuch der Paläeoherpetologie, Teil 19. Gustav Fisher, Stuttgart, 82 pp.

Wellnhofer P. (2001) - A Late Triassic pterosaur from the Northern Calcareous Alps (Tyrol, Austria). *Strata*, 11: 99-100.

Wellnhofer P. (2003) - A Late Triassic pterosaur from the Northern Calcareous Alps (Tyrol, Austria). In: Buffetaut E., Mazin J.-M. (Eds) - Evolution and palaeobiology of pterosaurs. *Geological Society of London, Special Publications*, 217: 5-22.

Wild R. (1975) - Ein Flugsaurier-Rest aus dem Lias Epsilon (Toarcium) von Erzingen (Schwäbische Jura). *Stuttgarter Beiträge zur Naturkunde* B, 17: 1-16.

Wild R. (1979) - Die Flugsaurier (Reptilia, Pterosauria) aus der Oberen Trias von Cene bei Bergamo, Italien. *Bollettino della Società Paleontolologica Italiana*, 17(1978): 176-256.

Wild R. (1994) - A juvenile specimen of *Eudimorphodon ranzii* Zambelli (Reptilia, Pterosauria) from the Upper Triassic (Norian) of Bergamo. *Rivista del Museo Civico di Scienze Naturali "E. Caffi" Bergamo,* 16(1993): 91-115.

Wiman C. (1925) - Über *Dorygnathus* and andere Flugsaurier. *Bulletin of the Geological Institut of Uppsala*, 19: 23-54.

Zambelli R. (1973) - *Eudimorphodon ranzii* gen. nov., sp. nov., uno pterosauro triassico. *Rendiconti dell' Istituto Lombardo di Scienze e Lettere, Classe di Scienze (B)*, 107: 27-32.